Meteorological catalysts of dust events and particle source dynamics of affected soils during the 1930s Dust Bowl drought, Southern High Plains, USA

Kasey Bolles[a,*], Mark Sweeney[b], Steven Forman[c]

[a] Division of Biology and Paleo Environment, Lamont-Doherty Earth Observatory, Columbia University, Palisades, NY 10964, United States
[b] Department of Sustainability & Environment, Earth Sciences Program, University of South Dakota, 414 E. Clark St., Vermillion, SD 57069, United States
[c] Department of Geosciences, Institute of Archeology, Baylor University, One Bear Place #97354, Waco, TX 76798, United States

ABSTRACT

Mineral dust aerosols are a key component of the Earth system and a growing public health concern under climate change, as levels of dustiness increase. The Great Plains in the USA is particularly vulnerable to dust episodes, but land-atmosphere interactions contributing to large-scale dust transport are poorly constrained. This study compiled one of the longest quantitative, spatially-comprehensive records of dust events in the core Dust Bowl region never before available. Combined with experiment station reports from the Soil Conservation Service, reanalysis data products, and contemporary field surveys using a Portable In-Situ Wind Erosion Laboratory (PI-SWERL), the study examined meteorological catalysts for dust events and surficial dynamics of particle emission on the Southern High Plains (SHP). Multivariate statistical analyses of dust event variance yield 6 principal components capturing ~60% of the variance of all dust event days. Results identified four dominant modes of dust events related to the season of occurrence and principal meteorological controls. A broader assessment of the potential emissivity of SHP soils reveals that disturbed surfaces begin to emit dust at a magnitude-higher rate than undisturbed surfaces as soon as the wind velocity reaches the threshold, increasing linearly with windspeed. Conversely, crusted undisturbed soil surfaces do not begin to reach the same flux rate until much higher windspeeds, at which point crusts are broken and emissivity rates increase exponentially. Significantly, the particle emissivity of undisturbed, loose sandy soils mirrors that of disturbed surfaces in relation to windspeed and potential magnitude of dust emission. This finding suggests that the prevalent sandier, rangeland soils of the SHP could be equal or greater dust sources than cultivated fields during periods of sustained, severe aridity.

1. Introduction

A persistent feature of 21st century climate forecasts is the increased frequency of droughts on the U.S. Great Plains, often with a severity and duration exceeding conditions of the 1930s Dust Bowl drought (DBD; e.g. Woodhouse et al., 2010; Cook et al., 2014, 2015; Pu and Ginoux, 2017). Past and future droughts on the Great Plains are associated with vegetation cover and land use changes, an increase in dust generation from denuded surfaces, and particle transport to nearby urban centers resulting in significant public health risks (Brown et al., 1935; Morman and Plumlee, 2013; Takaro et al., 2013; Goudie, 2014; Sprigg et al., 2014; Takaro and

Henderson, 2015). The Southern High Plains is a particularly potent source for atmospheric dust loading, likely to be exacerbated by competing agricultural and urban interests in water resources as drought intensifies (Basara et al., 2013; Cook et al., 2015). Historic records of drought in the past ca. 200 years document common large-scale dust events with the dense entrainment of mineral dust and other aerosols (Peters et al., 2007; Cook et al., 2009, 2013; Ravi et al., 2010), affecting air quality for a day to weeks at a time (Hand, 1934; Raman et al., 2014; Eagar et al., 2017). A deeper understanding of dust emission related to landscape denudation during the DBD, the last near continental-scale drought for North America (Cook et al., 2008, 2009), offers necessary context to better inform the extent, the severity, and the possible societal impacts of severe dustiness forecasted in the late 21st century (e.g. Pu and Ginoux, 2017).

The DBD was a time of elevated summer temperatures and pronounced deficits in evapotranspiration (Donat et al., 2016;

* Corresponding author.
E-mail address: kbolles@ldeo.columbia.edu (K. Bolles).

Cowan et al., 2017). Record-setting negative precipitation anomalies and agricultural practices across the Southern High Plains, a broad area including parts of northwest Texas and Oklahoma, northeastern New Mexico, eastern Colorado and west Kansas (Fig. 1a), led to surficial degradation and 1000s of dust events, particularly post-1933 (Joel, 1937; Cronin and Beers, 1937; Johnson, 1947; Chepil, 1957; Chepil et al., 1963; Bochert, 1971; Worster, 1979; Cunfer, 2005; Egan, 2006; Burnette et al., 2010;

Burnette and Stahle, 2013; Lee and Gill, 2015; Donat et al., 2016). Climate modeling studies and reanalysis of climate data places the DBD in a global context and underscores the complex land-ocean-atmosphere interactions propagating extreme droughts (Schubert et al., 2004; Fye et al., 2006; Cook et al., 2007; Seager et al., 2008; Cook et al., 2011; Nigam et al., 2011; Seager and Hoerling, 2014; Donat et al., 2016; Hu et al., 2018). However, there is insufficient knowledge of land surface processes, ecosystem changes,
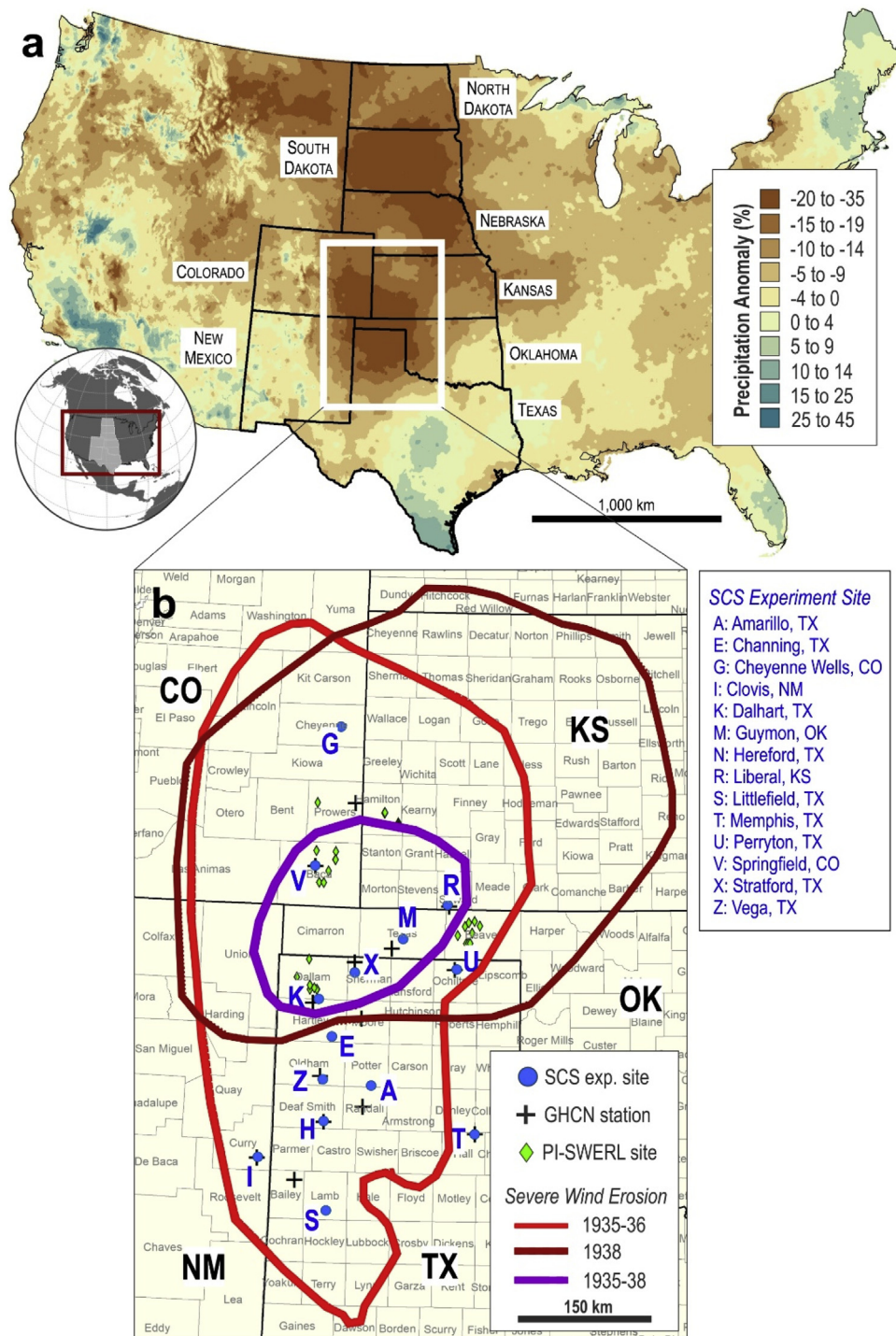
Fig. 1. Location of the Southern High Plains (SHP) and spatial distribution of observations incorporated in this study: (a) For the SHP (white box) precipitation anomalies during 1931–1940, indicate significantly drier conditions than during the previous 36-year period, 1895–1930 (calculated from PRISM Historical Past data series, http://prism. oregonstate.edu, created August 30, 2018), and (b) The locations of former Soil Conservation Service (SCS) experiment sites recording dust events, weather stations used from the Global Historical Climate Network (GHCN), and emissivity measurements recorded in the field with the PI-SWERL, in relation to the classically-defined severe wind erosion area (erosion boundaries redrawn from SCS map, dated March 1954, National Archives, Record Group 114, Entry 5).

atmospheric feedbacks, and concomitant physical controls on dust emissivity across the historically-defined Dust Bowl region (Fig. 1b; Cordova and Porter, 2015; Lee and Gill, 2015; Bolles et al., 2017; Bolles and Forman, 2018), which can limit climate model performance.

1.1. Mechanisms of dust particle generation and transport on the Southern High Plains

Dust emissions from mesic to semi-arid environments often reflect an interaction between extreme climate variability and human-induced landscape degradation, particularly since at least the early 20th century (Ginoux et al., 2012). Previous studies have examined individual dust events (e.g., Lee et al., 2012; Eagar et al., 2017), scrutinized synoptic climatology of dust events (e.g., Novlan et al., 2007; Knippertz, 2014), meteorological controls on atmospheric dust levels (e.g., Hahnenberger and Nicoll, 2012; Lei and Wang, 2014; Achakulwisut et al., 2017), and surface dust source extent and emissivity (e.g., Lee et al., 2009; Rivera Rivera et al., 2010; Sweeney et al., 2011; Flagg et al., 2014; Parajuli et al., 2014). Locally, dust emission is controlled by soil texture and moisture, surface roughness, the presence of soil crusts, wind-speed, gustiness, topography and vegetation cover, all of which are interdependent factors that respond nonlinearly to climate (Hugenholtz and Wolfe, 2005; Jickells, 2005; Engelstaedter et al., 2006; Werner et al., 2011; Houser et al., 2015). Changes to vegetation cover, soil moisture, and surface albedo may alter the atmospheric boundary layer, amplifying regional evapotranspiration and precipitation deficits and, most significantly for dust emission, mesoscale cyclonic disturbances sufficient to generate strong winds (Hahnenberger and Nicoll, 2012; Knippertz, 2014). Once entrained, the radiative effects of dust particles can modify the temperature gradient, pressure differential and local wind field, which then can alter cyclogenesis and rates of dust emission, transport and deposition across North America (Tegen et al., 1996; Boucher et al., 2013).

The semi-arid sandy rangelands of the Great Plains have not been considered as global sources of natural mineral dust; however, they are a significant source of anthropogenic dust (Ginoux et al., 2012). Sandy areas are frequently identified as a major contributor to regional dust aerosol loads (e.g. Bullard and White, 2005; Lee et al., 2009, 2012; Goossens and Buck, 2011; Sweeney et al., 2011, 2016a, 2016b; Crouvi et al., 2012). The landforms most prone to natural dust emission contain abundant sand sources, and such surfaces begin to emit dust at lower friction velocities compared to crusted soils with higher silt content (Gillette et al., 1980; Sweeney et al., 2011; Flagg et al., 2014). Sandy soils, such as those that predominate the Southern High Plains, commonly emit dust during sustained and high magnitude events via mechanisms that include saltation bombardment on a fine-grained substrate (Shao et al., 1993; Lee et al., 2009) and release of fines contained within sand deposits (Sweeney et al., 2016a). Chipping and spalling of sand grains during ballistic impact and removal of grain coatings can produce low levels of dust (Bullard and White, 2005; Huang et al., 2019; Swet et al., 2019), but in some cases can become significant over large areas of active dunes (Crouvi et al., 2012). These micro-scale mechanisms, when combined with severe drought conditions, have the potential to cause magnitude increases in the production of mineral dust aerosols. Though dust emission can be short-lived and occur in isolation, often it is part of a succession of events leading to large-scale dust episodes spanning hours to days, with continental-scale impacts (Donarummo, 2003; Peters et al., 2004, 2007; Knippertz, 2014).

Meteorological conditions (Rivera Rivera et al., 2009; Lei and Wang, 2014; Raman et al., 2014; Achakulwisut et al., 2017; Tong

et al., 2017), synoptic pressure gradients (Wigner and Peterson, 1987; Knippertz, 2014), and land-atmosphere feedbacks (Cook et al., 2009; Hu et al., 2018) contribute to the scale and intensity of dust emission. The most vigorous dust event, or *haboob*, (Sutton, 1931; Idso et al., 1972; Williams et al., 2009) generally forms with the passage of a steep front and a sustained, deep low-pressure system that induces intense atmospheric convection over a sparsely vegetated terrain (Sidwell, 1938; Smith et al., 1970; Idso et al., 1972; Chen and Fryrear, 2002; Novlan et al., 2007). Haboobs in the western U.S. are often characterized by a dense dust-cloud associated with Mesoscale Convective Complexes or cold fronts (Idso et al., 1972; Patterson and Gillette, 1976; Maddox, 1983; Lee and Tchakerian, 1995; Novlan et al., 2007; Camino et al., 2015; Lee and Gill, 2015; Baddock et al., 2016; Eagar et al., 2017). Eastward shifts of atmospheric dust concentrations and zones of light dust air-fall across the Midwest during the DBD extended nearly to the eastern seaboard, reflecting the passage of such dust-laden low-pressure systems (Handy et al., 1960; Brown et al., 1968; Namias, 1982; Mo et al., 1997).

Poor agricultural stewardship has been designated as the major cause for widespread landscape denudation during the DBD, which purportedly left cultivated areas barren and exposed to eolian erosion (e.g. Bennett and Fowler, 1936; Johnson, 1947; Worster, 1979; Hurt, 1981; Hansen and Libecap, 2004). The still photographic record captured during the 1930s under the auspices of the Farm Security Administration (Ohm, 1980; Lange, 1981; Packer, 2011), showed desolate fields covered by wind-rippled sands, and dunes that engulfed homes, out buildings, fields and fence-lines (Fig. 2). This photographic record documented in some areas the severity of land surface responses to intense drought and was evoked to characterize the geomorphic consequence of the Dust Bowl (cf. Lockeretz, 1978; Riebsame, 1986; Lookingbill, 2001; Porter and Finchum, 2009; Porter, 2012; Duncan and Burns, 2012). However, analyses of historical agricultural census data underscores that just one-third of the Great Plains was under cultivation in the 1930s, and poor agricultural practices have been questioned as the sole cause for soil loss (cf. Cunfer, 2005; Hornbeck, 2012; Sylvester and Rupley, 2012). Closer scrutiny of agricultural treatments in an analysis of mosaicked aerial photographs from the 1930s across Kansas concluded that the misuse of land unsuitable for cultivation was relatively rare (Sylvester and Ripley, 2012). Additionally, stratigraphic studies documented partial reactivation of stabilized dune fields during the 1930s in western Kansas (Forman et al., 2008; Bolles et al., 2017). Aerial photographs acquired during the 1930s have revealed many areas of active eolian sediment transport in rangelands, revealing natural and anthropogenic dust sources during the Dust Bowl (Bolles et al., 2017; Bolles and Forman, 2018).

1.2. Data constraining the distribution and character of the 1930s dust events on the Great Plains

There are few localities with continuous records of dust events for the 20th century on the Great Plains, and fewer that provide detailed quantitative data on dust events during the 1930s (Lee and Tchakerian, 1995). Records for Dodge City and Garden City, KS show peak occurrence at 100 to 120 dust events per year from 1936 to 1939 (Fig. 3a), a ten-fold increase compared to the wettest periods of the 1920s and 1940s, with an average of <10 events per year (Orgill and Sehmel, 1976). A similar "background" dust event frequency was documented for Lubbock, TX between 1942 and 1965, with the threshold for dust event identification at a visibility of ≤10 km (Orgill and Sehmel, 1976), a somewhat higher threshold than many DBD metrics. The highest frequency of dust events in the 1930s occurred preferentially in the spring, usually during April and May (Fig. 3b) with the increased west to east passage of
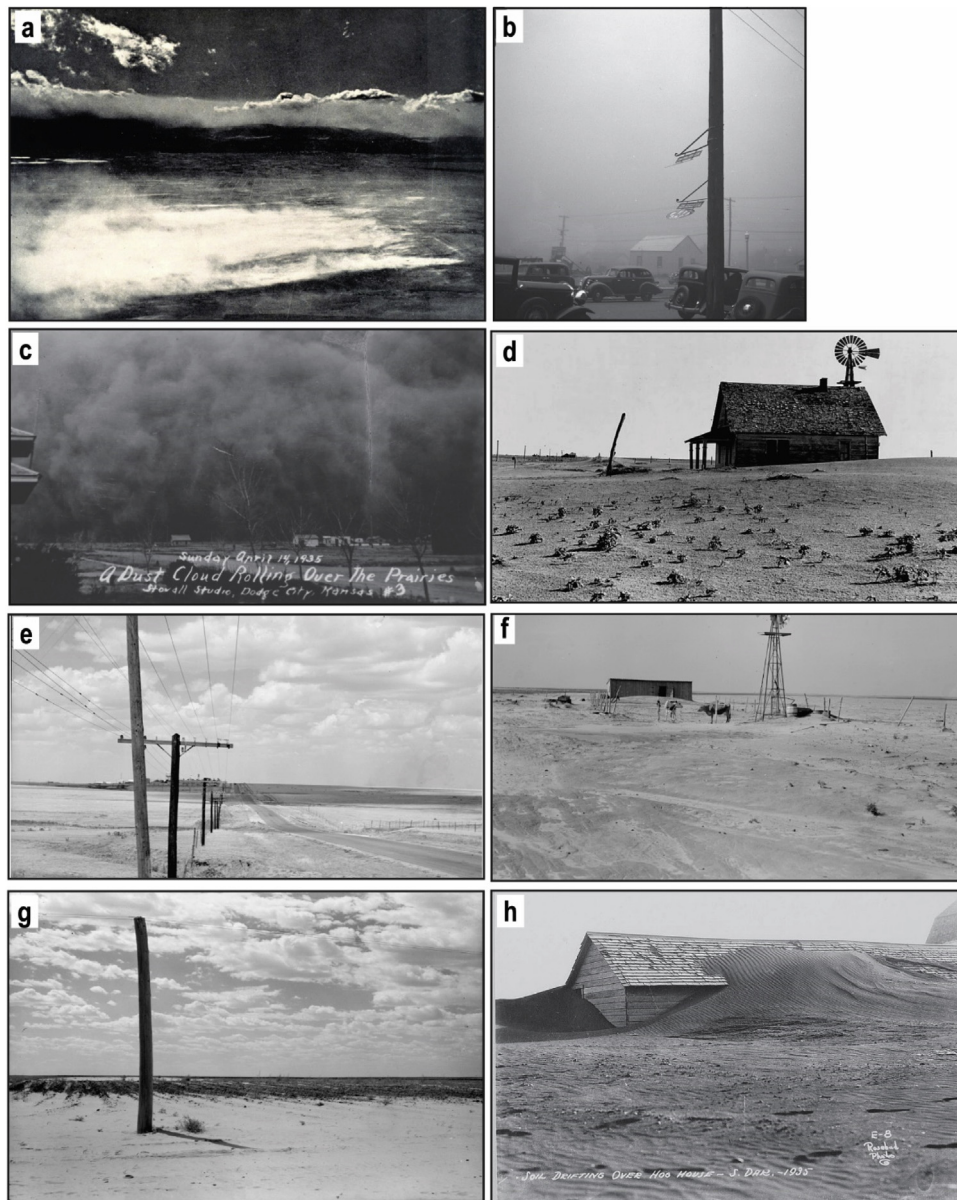
Fig. 2. Dust Bowl Drought still photographic record; (a) Aerial view of the beginning of a dust storm over the Piedmont west of Denver (from Choun, 1936, p. 197). (b) Dust storm in Amarillo, TX, April 1936, photographed by Arthur Rothstein (Farm Security Administration [FSA], National Archives, Digital I.D. 8b27557). (c) The dust storm on Black Sunday April 14, 1935, near Hugoton, KS (accessed from: http://www.kansasmemory.org/item/323). (d) Dust Bowl farm in the Coldwater District, north of Dalhart on June 1938, taken by Dorothea Lange (FSA, National Archives, Digital I.D. 8b32396). (e) Great Plains and highway north of Amarillo, TX, August 1938 taken by Dorothea Lange (FSA, National Archives, Digital I.D. 8b34910). (f) Barn and shed of farm in the Texas Panhandle near Boise City, TX on 1938 June taken by Dorothea Lange (FSA, National Archives, Digital I.D. 8b38680). (g) View near Dalhart, TX of plants and sand on July 1936, taken by Arthur Rothstein (FSA, National Archives, Digital I.D. 8b28143). (h) Soil drifting over hog house, South Dakota (FSA, National Archives, Digital I.D. 8e03187).

cyclonic disturbances (cf. Schubert et al., 2004; Novlan et al., 2007), a similar pattern to dust event occurrence between 1942 and 1970 (Orgill and Sehmel, 1976) and recent decades (Lee and Tchakerian, 1995; Novlan et al., 2007) for the conterminous U.S.. A secondary peak in dust event activity occurred in January with a preponderance of dust events (>30%) when visibility was <1.6 km (Fig. 3b), which also mirrors broader trends for dust event occurrence post-DBD across the U.S. (Orgill and Sehmel, 1976; Wigner and Peterson, 1987; Lee and Tchakerian, 1995).

There is limited data on dust concentrations and deposition rates for the Great Plains during the 1930s, though there are multiple sources of dust recognized across the DBD landscape (Lee and Gill, 2015). The most common dust deposition measurements were completed post passage of a dust event as deposited thicknesses of sediment for a known area over a period of time, usually within 24 h (Table 1). These measurements included sediment thicknesses for deposits on agricultural fields, within flat "Texas" cake-baking pans placed on elevated areas (usually roof tops) prior to passage of an event, and particulates accumulated in rain gauges. A few pioneering scientific studies in the 1930s used the available dust sampling technology to quantify atmospheric particulate flux, such as an Owens Dust Counter (Hand, 1934) or an Impinger Tube (Langham et al., 1938). The study by Langham et al. (1938) is of significance because of the continuous measurement of dust flux, windspeeds, and visibility for twenty-nine dust events from April 1935 through April 1937 at the core of the DBD in Goodwell, OK (Table 1). Total suspended particle concentrations for individual dust events vary from 0.1 to 4.0 g m^{-3} (Langham
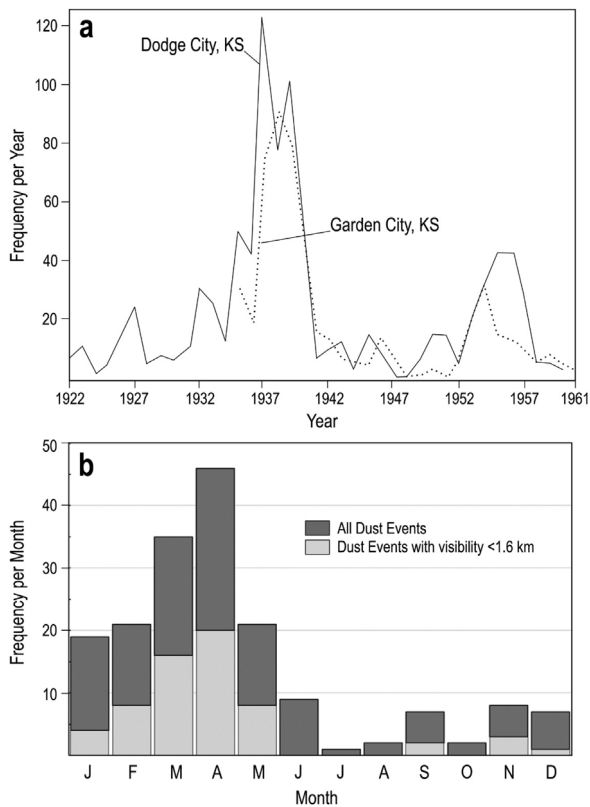
Fig. 3. (a) Annual dust storm frequency for Dodge City and Garden City, KS between 1922 and 1961 (from Chepil et al., 1963); and (b) monthly dust storm frequency from 1933 to 1936 for Amarillo, TX (compiled from Choun, 1936; Joel, 1937).

et al., 1938) and were similar in magnitude to contemporary dust events sourced from North Africa and the southwestern U.S., with visibility often below 0.5 km and advancing "wall" of dust rising 2 to 4 km in height (Langham et al., 1938; Englestaedter et al., 2006; Rivera Rivera et al., 2010; Flagg et al., 2014; Camino et al., 2015; Eagar et al., 2017).

Monthly maps showing the spatial distribution of dust event days and/or "dense dust" atmospheric conditions of the conterminous U.S. provide insight on the cross-continent impact of suspended dust loads prior to the study period (Fig. 4). These maps indicated a concentration of dusty days centered over the Texas and the Oklahoma panhandles, though the loci of dust events shifted northward into southwest Kansas from March to May in 1936 (Fig. 4d-f). Another dust source accentuated in the maps was on the northern Great Plains, with peak dusty conditions over the North and South Dakota border area from May 1934 to February 1935, and again June 1936 (Fig. 4a, g). Noteworthy is the westward distribution of dust observed in March 1936 that fell in the southern Basin and Range and Northern Rocky Mountains, with an eastward displacement of an upper level ridge (Fig. 4d; Namias, 1982, 1990; Higgins et al., 1997). It appears that broad areas of the Great Plains were dust sources in the 1930s, which could be redistributed eastward or westward with changing synoptic conditions, such as a dust event occurring November 12 to 13, 1933 that produced dustfall across the eastern U.S. (Fig. 5). In addition, there may be numerous unrecognized secondary sources for dust emissivity from extensively plowed fields in the Midwest and over-utilized pasture lands west of the Front Range (Handy et al., 1960; Brown, 1968).

This study attempts to combine meteorological and land surface observations from the 1930s with contemporary field surveys and measurements to better define the variance in

Southern High Plains dust activity during the DBD. We seek to address three over-arching questions:

(1) What meteorological and/or land surface conditions principally influence the variability of dust events associated with this prolonged period of aridity?
(2) Are there seasonal trends in dust event occurrence related to weather patterns and/or land surface conditions within the classically-recognized Dust Bowl region?
(3) How does the surficial emissivity of potential dust sources across the Southern High Plains differ by soil texture, and by what magnitude does anthropogenic disturbance impact particle flux from soils of varying particle size distributions?

2. Methods

To explore dynamics of dust activity associated with the Dust Bowl, a daily record of dust events between April 1938 and May 1940 was compiled from archival records of SCS experiment stations (National Archives, Record Group 114), one of the longest quantitative and spatially-comprehensive records of dust events in the core Dust Bowl region never before available. Coeval meteorological conditions retrieved from the Global Historical Climate Network (Menne et al., 2012), and the 20th Century Reanalysis Project (Compo et al., 2011) enabled multivariate statistical analyses of event occurrence based on parallel covariance, illuminating common catalysts on dust event days and how those mechanisms vary seasonally. Finally, the relative contribution of available particle sources to Southern High Plains dust events is assessed based on the magnitude of surficial particulate matter (PM_{10}) flux as a function of windspeed, measured in the field from soil surfaces across different soil textures and land uses analogous to the 1930s.

2.1. Archived records of the Soil Conservation Service

The Soil Conversation Service (SCS) established a series of soil experiment stations focused on developing new methods to prevent eolian erosion, runoff, and stabilize blowing soils to mitigate the environmental and economic devastation of the Dust Bowl Drought (DBD). The archived records from these experiment stations span from 1929 to 1942 and yield detailed accounts of land surface conditions at the township scale. In particular, these records reveal for the 1930s annual changes in soil and water conservation practices, observations on vegetation type, cover, and distribution, tillage operations, documentation of erosion and revegetation of abandoned fields, still photographs, and field-level erosion maps. This study utilized records from four experiment stations in Fort Hays, KS, Elkhart, KS, Amarillo, TX, and Dalhart, TX. Records from the Dalhart SCS substation, where data was centralized from dozens of smaller experimental sites, offer a particularly comprehensive record of dust movement from 1937 to 1941. Hardcopy "Dust Storm Data" reports from these sites provide a continuous, quantitative inventory of dust events at the center of the traditionally-drawn Dust Bowl boundaries (Fig. 1b), collated and digitized for the first time in this study. Recorded parameters include the month, day, start and end time of each event, the associated visibility, maximum wind velocity and direction during the event, and severity of soil damage observed with the passage of each event.

This study focused on data from April 1938 to May 1940 because at least 80% of experimental sites submitted monthly data series during this period and thus minimizes the error introduced by inconsistent reporting and/or missing datasheets. This 26-month period coincides with the peak activity in dust events recorded at

Table 1
Estimated wind speed, visibility, dust deposition rate and total suspended sediment for dust storms during the 1930s.

Date	Location	Measurement method	Wind speed (m s⁻¹)	Visibility (km)	Estimated dust deposition rate (g m⁻² hr⁻¹)	Sample duration (hr)	Estimated TSP (g m⁻³)	Data Source
05/11/1934	Washington, D.C.	Owens dust counter			3.6	9.75		Hand, I., 1934
03/15/1935	Jewell CO, KS	Wet bake pan			⁻19.4	24		Brown et al., 1935
03/26/1935	Jewell CO, KS	Wet bake pan			⁻10.4	24		Brown et al., 1935
03/26/1935	Jewell CO, KS	Rain gauge			⁻9.3	24		Brown et al., 1935
04/26/1935	Jewell CO, KS	Wet small pan			⁻4.2	24		Brown et al., 1935
04/22/1935	Jewell CO, KS	Wet small pan			⁻1.2	24		Brown et al., 1935
04/04/1936	Goodwell, OK	Impinger tube	10 ± 2	0.1	2.5 ± 0.6	0.75	2 ± 0.4	Langham et al., 1938
04/05/1936	Goodwell, OK	Impinger tube	12 ± 1	0.1	1.4 ± 0.2	1	1.4 ± 0.2	Langham et al., 1938
04/08/1936	Goodwell, OK	Impinger tube	11 ± 1	0.6 ± 0.2	0.3 ± 0.1	1.5	0.3 ± 0.1	Langham et al., 1938
04/09/1936	Goodwell, OK	Impinger tube	14 ± 1	0.1 ± 0.1	2.8 ± 0.8	0.75	2.2 ± 0.6	Langham et al., 1938
04/20/1936	Goodwell, OK	Impinger tube	13 ± 1	0.1	6.0 ± 2.8	0.6	3.6 ± 1.7	Langham et al., 1938
04/23/1936	Goodwell, OK	Impinger tube	11 ± 8	0.6 ± 0.3	0.06 ± 0.01	5.2	0.3 ± 0.1	Langham et al., 1938
04/29/1936	Goodwell, OK	Impinger tube	9 ± 2	0.5 ± 0.2	0.15 ± 0.08	1.3	0.2 ± 0.1	Langham et al., 1938
05/05/1936	Goodwell, OK	Impinger tube	10 ± 1	0.2 ± 0.2	0.42 ± 0.21	2.4	1 ± 0.5	Langham et al., 1938
05/08/1936	Goodwell, OK	Impinger tube	10 ± 1	0.1	2.0 ± 0.7	1.2	2.4 ± 0.8	Langham et al., 1938
02/1937	Page CO, Iowa	Observation			⁻1.3	24		Martin, 1937a
02/1937	Sault. Ste. Marie, MI	Observation			⁻0.2	24		Martin, 1937a
02/1937	Marquette, MI	Observation			⁻0.07	24		Martin, 1937a
02/07/1937	Goodwell, OK	Impinger tube	13 ± 1	0.1 ± 0.1	0.24 ± 0.02	8.3	2 ± 0	Langham et al., 1938
02/11/1937	Goodwell, OK	Impinger tube	10 ± 1	0.4	0.05 ± 0.01	3.75	0.2 ± 0	Langham et al., 1938
02/14/1937	Goodwell, OK	Impinger tube	11 ± 1	0.1 ± 0	0.20 ± 0.12	6.75	1.3 ± 0.8	Langham et al., 1938
02/15/1937	Goodwell, OK	Impinger tube	8 ± 0.4	0.3 ± 0.1	0.03 ± 0.02	6.3	0.2 ± 0.1	Langham et al., 1938
02/16/1937	Goodwell, OK	Impinger tube	11 ± 1	0.3 ± 0.4	0.24 ± 0.19	7.2	1.7 ± 1.4	Langham et al., 1938
02/17/1937	Goodwell, OK	Impinger tube	10 ± 1	0.1 ± 0.1	0.05 ± 0.03	6.2	0.3 ± 0.2	Langham et al., 1938
02/18/1937	Goodwell, OK	Impinger tube	14 ± 0	0.1 ± 0.1	0.82 ± 0.73	2.2	1.8 ± 1.6	Langham et al., 1938
03/03/1937	Goodwell, OK	Impinger tube	9 ± 3	0.2 ± 0.1	0.03 ± 0.01	10.3	0.3 ± 0.1	Langham et al., 1938
03/09/1937	Goodwell, OK	Impinger tube	10 ± 1	0.4 ± 0.3	0.20 ± 0.1	4	0.7 ± 0.4	Langham et al., 1938
03/17/1937	Goodwell, OK	Impinger tube	8 ± 1	0.4 ± 0	0.10 ± 0.01	1.75	0.2 ± 0	Langham et al., 1938
03/19/1937	Goodwell, OK	Impinger tube	10 ± 1	0.1 ± 0.1	1.4 ± 0.5	6	1.4 ± 0.5	Langham et al., 1938
03/23/1937	Goodwell, OK	Impinger tube	13 ± 1	0.1 ± 0	0.30 ± 0.01	13.7	4 ± 1.1	Langham et al., 1938
03/24/1937	Goodwell, OK	Impinger tube	9 ± 1	0.1 ± 0.1	0.01 ± 0.01	11.3	1.5 ± 0.9	Langham et al., 1938
04/02/1937	Goodwell, OK	Impinger tube	8 ± 2	0.5 ± 0.3	0.05 ± 0.01	8.4	0.4 ± 0.2	Langham et al., 1938
04/03/1937	Goodwell, OK	Impinger tube	6 ± 1	0.4 ± 0.1	0.04 ± 0.01	5	0.2 ± 0.1	Langham et al., 1938
04/06/1937	Goodwell, OK	Impinger tube	11 ± 1	0.1 ± 0.1	0.2 ± 0.1	5	1 ± 0.6	Langham et al., 1938
04/16/1937	Goodwell, OK	Impinger tube	9 ± 1	0.2 ± 0.1	0.05 ± 0.01	8	0.4 ± 0.2	Langham et al., 1938
04/22/1937	Goodwell, OK	Impinger tube	9 ± 1	0.1 ± 0.1	0.2 ± 0.1	5	1.1 ± 0.5	Langham et al., 1938
04/23/1937	Goodwell, OK	Impinger tube	9 ± 2	0.3 ± 0.3	0.2 ± 0.1	5.6	1.2 ± 0.7	Langham et al., 1938
4/27/1937	Fort Collins, CO	Observation			⁻6.1	24		Martin, 1937a
05/03/1937	Goodwell, OK	Impinger tube	10 ± 1	0.4 ± 0.2	0.05 ± 0.02	11	0.5 ± 0.2	Langham et al., 1938

other locations, such as Dodge City and Garden City, KS (Fig. 3a), and with severe drought conditions in the Oklahoma and Texas panhandles where mean Palmer Drought Severity Index values were <-3 during 1939 and 1940 (Bolles and Forman, 2018, Fig. 3). Whereas local-scale land surface conditions and land use varied interannually during the 1930s, meteorological drivers of dust emission would not change significantly given the persistence of circulation anomalies between 1932–1939 (Cook et al., 2011). Thus, dust events in this study period were dynamically similar to dust activity from earlier in the decade. Surface conditions during dust events pre-1937 were potentially divergent from our study period, as the distribution of surficial dust sources expanded rapidly between 1933 and 1937, when vegetation loss plateaued at its maximum spatial extent (Joel, 1937; Albertson and Weaver, 1942). However, ecological studies documented delayed rangeland recovery until normal precipitation levels returned in 1941 (Albertson and Weaver, 1942, 1944), and therefore dust events in 1937–1940 are considered here to be generally representative of the cumulative effect of the Dust Bowl phenomenon on the Southern High Plains.

2.2. Statistical analyses of dust event variability

Multivariate statistical analyses were utilized to decompose dust event variance during the study period, which were computed on a matrix of 31 variables for 1018 dust events

(Table 2). Dust events with missing values were excluded from this portion of analysis to ensure data standardization without undue skewing. A pairwise correlation using Spearman's Rho (R_S) was calculated to explore the strength and direction of dependence between the rank order of variable pairs, with an R_S over ± 0.8 and a p-value ≤0.05, indicative of a strong monotonic relation (Borradaile, 2003). A principal component analysis (PCA) of the same matrix revealed the strength and direction of variable covariance, and the subsequent principal components (PCs) are mutually uncorrelated (Wilks, 2011). We considered individual PCs explaining at least 5% of the variance to have a substantial correlation to the distribution of dust events. The specific eigenvectors most closely associated with each PC above this 5% threshold were identified within the 90th percentile of absolute variable coefficients. Seven distance metrics were computed between event observations to determine the hierarchical cluster tree(s) with the strongest cophenetic correlation (Wilks, 2011), as evaluated by Euclidean, squared Euclidean, correlation, cosine, city block, hamming, and Spearman's linkages. To characterize common dust event modes the number of PCs needed to explain 90% of the variance was set as the maximum number of clusters, with linked cluster tree nodes aggregated to the number of PCs needed to explain 50% of the variance. Finally, meteorological anomalies on dust event days were calculated in reference to mean conditions on days without dust events within the same season.
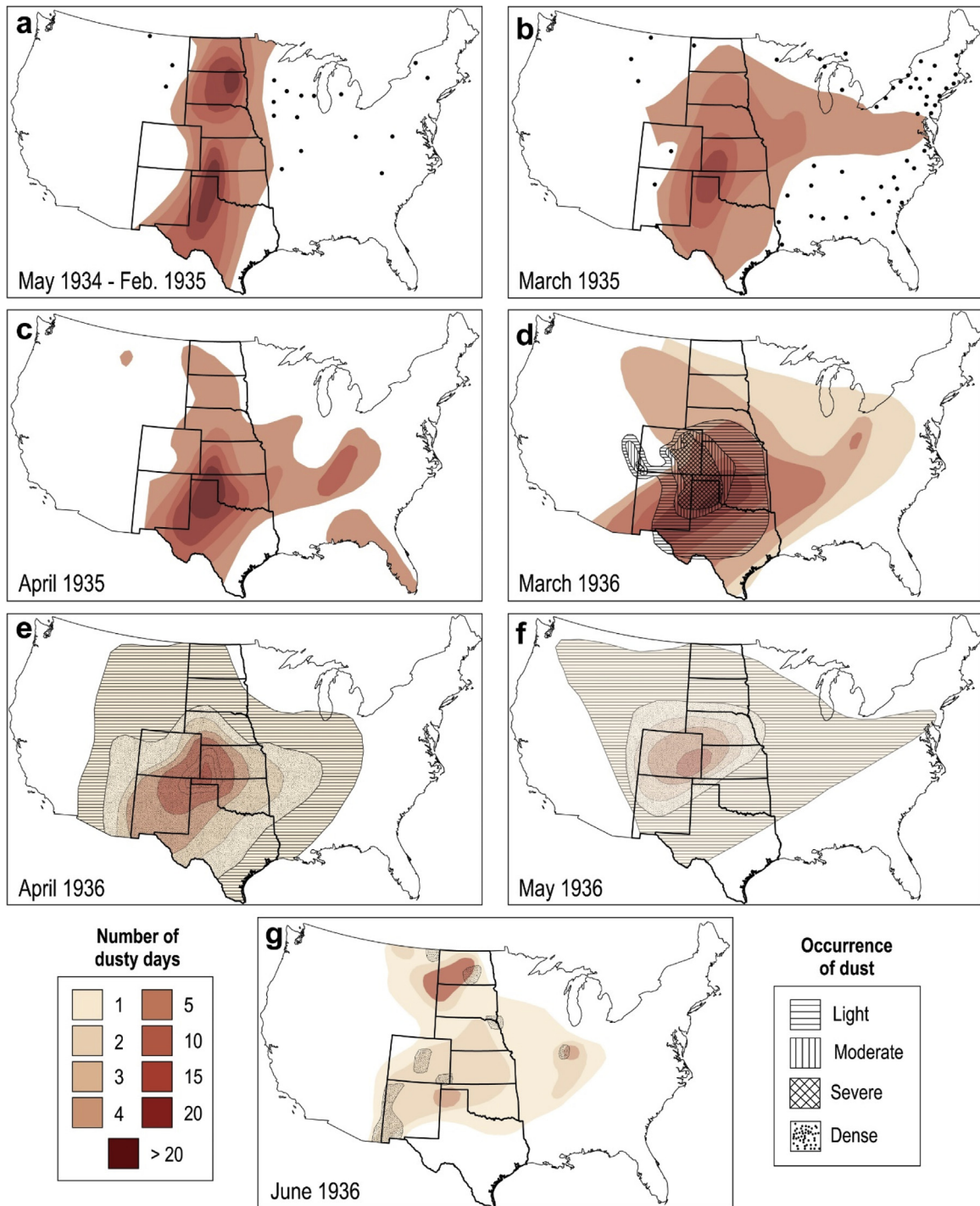
Fig. 4. Spatial distribution of dust storms and dust occurrence for designated months in 1934, 1935 and 1936 (from Mattice, 1935a, 1935b; Choun, 1936; Martin, 1936a, 1936b, 1936c).

2.3. Assessment of potential emissivity from modern analogous surfaces

The Portable *In-Situ* Wind Erosion Lab (PI-SWERL; Etyemezian et al., 2007) measures the potential of soil surfaces to emit dust. Dust emissions from the PI-SWERL are equitable to large field wind tunnels (Sweeney et al., 2008) and it has been tested on a variety of geomorphic surfaces (Bacon et al., 2011; Goossens and Buck, 2009; King et al., 2011; Sweeney et al., 2011, 2016a, 2016b; Sweeney and Mason, 2013). In the field, 139 sites were measured from a spectrum of analogous soil surfaces ranging in texture from silt-

loam to sand, derived from Late Pleistocene to Holocene eolian and/or fluvial deposits. Sites were distributed across land use and landforms on: 1) active dune sand, 2) stabilized dune sand, 3) buried soils developed in eolian sand, 4) sandsheet areas, 5) cultivated areas, both fallow and actively used, of eolian (loess) or fluvial origin. We recognize that our test sites do not reflect exact conditions of the soil during the 1930s due to wind erosion that resulted in localized changes in soil texture and ensuing intensive agricultural use. However, given that across the region there are "extensive areas of quite uniform soils, slopes, and native vegetation [. . .] with similar erosion susceptibility" (Joel,
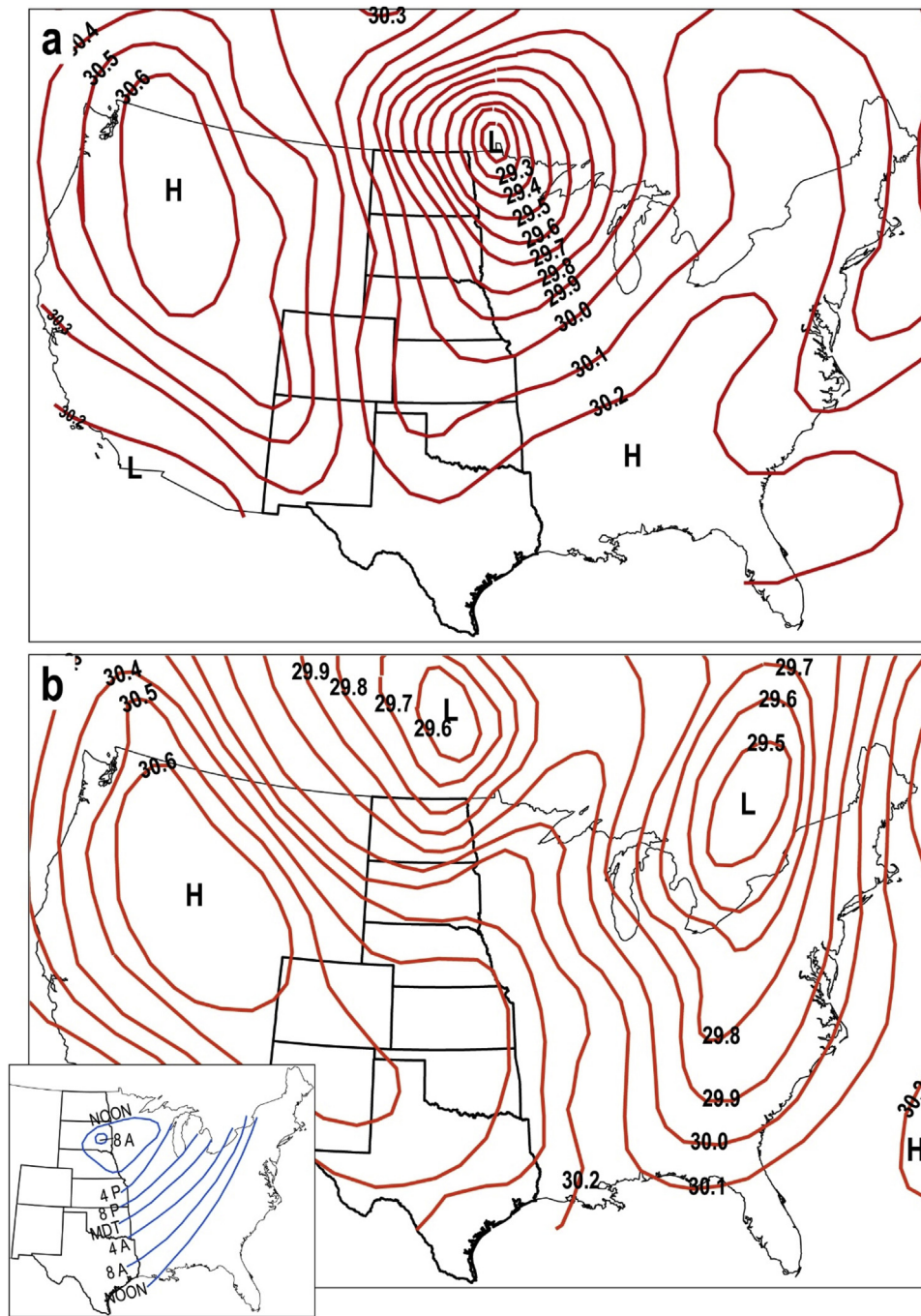
Fig. 5. (a) Weather map for 8 a.m. November 12th, 1933 and (b) 8 a.m. on November 13th (bottom), when dustfall occurred from eastern Ontario, across western New York, the Ohio River Valley, the southern Appalachians and the Gulf States to Texas. Inset map shows isochronal contours for the movement of dust clouds for the same 24-h period (Miller, 1934).

1937), and that the soil texture of the dominant soil series varies nominally with depth through the B-horizon (Turnure, 1938; Soil Survey Staff, 2019), our sites are analogous to soil textures subject to eolian erosion in the 1930s at the landscape-scale any given point in time during the drought (cf. Bolles et al., 2017; Bolles and Forman, 2018). We excavated ca. 1930s paleosols in dune sand for PI-SWERL testing, and also tested B-horizons in agricultural lands, likely exposed by severe wind erosion. A hand cultivator was used to pulverize soil crusts and aggregates for "disturbed" surface tests to simulate the effect of tillage on dust emission, particularly "listing," a documented practice in the 1930s that enhanced particle flux (Lee and Gill, 2015). At each site a bulk soil sample was

collected for particle size analysis by laser diffraction with a Malvern Mastersizer 2000.

The PI-SWERL contains an annular blade in an enclosed 0.5 m diameter cylindrical chamber, open to the ground surface, that rotates at prespecified speeds that are equated to friction velocities (u^*, m s^{-1}). For each test, the rotation speed was increased in a step-wise fashion and held constant at each RPM step (typically from 2000, 3000, 4000, and 5000 RPM) for 60 s to measure the response of the surface to different friction velocities. A DustTrak II aerosol monitor (TSI, model 8530) measures the concentration of PM$_{10}$ dust emitted during testing in mg m^{-3}. Dust concentrations are converted to a dust emission rate (mg m^{-2} s^{-1}) using the area

Table 2
Notation, description, and data source of the 31 variables included in statistical analyses.

Notation	Description	Unit	Data Source
stormID	Recording location and date	—	National Archives, Record Group 114, Entry 112, File:
Season	Season of event occurrence	1: MAM	Dust Storm Data Sheets
		2: JJA	
		3: SON	
		4: DJF	
sHOUR	Hour of day event began	—	
eHOUR	Hour of day event ended	—	
Dur	Total daily duration	Hours	
mDur	Multi-day duration		
Vis	Visibility (Light, Moderate, Dense)	L: 1.2 to 9.5 km	
		M: 0.3 to 1.2 km	
		D: <0.3 km	
WS	Maximum wind velocity observed during event	m s^{-1}	
WD1	Predominant wind direction during event	°Azimuth	
Dam	Level of reported soil damage caused by event	1: Slight	
		2: Moderate	
		3: Severe	
tMIN	Daily minimum temperature	°C	Global Historical Climate Network (Menne et al., 2012)
tMAX	Daily maximum temperature	°C	
tMEAN	Daily mean temperature	°C	
ppt	Daily rainfall	mm	
pptLast	Time since last rainfall	Days	
pDiff	% difference in total monthly rainfall from 1895-1930 mean	%	PRISM Historical Data Series (PRISM, 2017)
perCult	% of county cultivated by 1935	%	Agricultural Census of 1935 (Gutmann, 2005)
perDune	% of county mapped as eolian deposits	%	Muhs and Holliday (2001)
rCAPE	Convective available potential energy	J kg^{-1}	20th Century Global Reanalysis Project (Compo et al., 2011)
rEVBS	Direct evaporation from bare soil	W m^{-2}	
rPET	Potential evapotranspiration	W m^{-2}	
rPS	Surface air pressure	Pascal	
rPWAT	Atmospheric water vapor content	kg m^{-2}	
rRH850	Relative humidity at 850 hPa	%	
rSHUM	Specific humidity at 2m	kg kg^{-1}	
rSM	Soil moisture content	kg m^{-2}	
rT2M	Daily mean air temperature at 2m	°K	
rT850	Daily mean air temperature at 850 hPa	°K	
rUWIND10	u-wind at 0.995 times the surface pressure	m s^{-1}	
rVWIND10	v-wind at 0.995 times the surface pressure	m s^{-1}	
rWS10	Wind speed at 10m	m s^{-1}	
rZ1000	Geopotential height at 1000 hPa	m	
rZ500	Geopotential height at 500 hPa	m	
rZ200	Geopotential height at 200 hPa	m	

under the annular blade, duration of the test, air flow rate, and dust concentration (Sweeney et al., 2008). The friction velocities exerted by the PI-SWERL assume a smooth surface, so a surface roughness correction must be applied (Etyemezian et al., 2014). The surface roughness correction, alpha (α), is chosen from a look-up table based on grain size of the soil surface, the presence of a smooth or rough crust, stones, or soil clods. Values range from 0.84 to 0.98, with 1.0 equaling a perfectly smooth surface (Table 3).

To equate PI-SWERL friction velocities to 2-m windspeeds, we applied the "law of the wall" and estimated landscape-scale surface roughness values (Table 3). Surface roughness lengths for sand dunes was estimated at 0.00023 m (Oke, 1978; Gillette et al., 1982; Lancaster, 2004), and bare to sparsely vegetated agricultural fields were estimated at 0.0005 m (Gillette, 1988). Flux curves for a particular surface type were derived from goodness-of-fit tests for exponential and quadratic polynomial functions, with and without robust bi-square fitting. Iterative experimentation demonstrated these models provided more accurate fits than linear polynomial and power law functions. Initial coefficients were estimated from the fit tests and used in model runs to determine the regression with the lowest root mean squared error (RMSE) and functional simultaneous 95% confidence intervals. Where the RMSE between models is equal or nearly equal, the regression returning the lowest mode value of residuals was selected. The final flux models were applied in a case study of the Dalhart Sand Dunes Area, in Dallam County, Texas, to assess the potential contribution of PM$_{10}$ from different soil surfaces to an observed dust event that occurred on April 7, 1937. Surface conditions were derived from an aerial photograph taken October 5, 1936, digitized from original reel film held at the National Archives in College Park, MD. Soil texture was ascertained from Soil Conservation Service records (Eby and Whitfield, 1940) and verified with the Web Soil Survey (Soil Survey Staff, 2019). Potential dust emissions were modeled after Bolles et al. (2017).

3. Results

The fourteen Soil Conservation Service (SCS) experiment sites reported 1360 events between April 1938 and May 1940, lasting a total of 9,603 h – nearly 50% of the elapsed time (Table 4). Dust activity peaked in the spring with a maximum in frequency each April (Fig. 6a), mirroring records from earlier in the decade (Fig. 3b). The events with the greatest reduction in visibility were most frequently associated with northerly winds, whereas the events resulting the most severe soil damage were most frequently associated with southwesterly winds. The greatest number of consecutive days with dust events in the study period was documented in Springfield, CO (Fig. 7, site V), where dust blew for 18 days from April 1st to 18th, 1938 for a total of 128 h (30% of the period), shortly followed by a further nine consecutive days of dust events from April 21st to 29th, for an elapsed time of 56 h. The longest individual event persisted for 98 h, also recorded in

Table 3
Alpha (α) coefficients and PI-SWERL friction velocities corrected for surface roughness and estimated 2 m wind speeds (m s^{-1}).

α	Soil Condition	Landscape Roughness length z_o, m	2000 RPM		3000 RPM		4000 RPM		5000 RPM	
			u*	2-m	u*	2-m	u*	2-m	u*	2-m
1.00	—	N/A	0.38		0.53		0.68		0.82	
0.98	Smooth crust, Very fine sand	0.0005	0.40	8.29	0.56	11.7	0.72	14.93	0.87	18.05
0.96	Loose fine-medium sand	0.00026	0.42	9.42	0.60	13.39	0.77	17.18	0.93	20.84
0.96		0.0005	0.42	8.73	0.60	12.41	0.77	15.92	0.93	19.32
0.94	Rough Crust, Medium-coarse sand	0.0005	0.45	9.2	0.64	13.22	0.82	17.05	1.00	20.78
0.92	Crust with small clods	0.00026	0.47	10.51	0.68	15.27	0.89	19.8	1.08	24.23
0.92		0.0005	0.47	9.81	0.68	14.15	0.89	18.36	1.08	22.46
0.9	Sand with small clods	0.0005	0.50	10.37	0.73	15.22	0.96	19.86	1.18	24.41
0.86	Stones or Clods, 1-4 cm	0.00026	0.58	13.05	0.86	19.32	1.14	25.52	1.42	31.67
0.86		0.0005	0.58	12.1	0.86	17.91	1.14	23.65	1.42	29.35
0.84	Clods, 4-5 cm	0.0005	0.63	13.1	0.95	19.7	1.26	26.2	1.57	32.6

Table 4
Locations of Soil Conservation Service experiment sites recording dust storms used in this study and total number of storms and duration documented from April 1938 to May 1940, inclusive.

Notation	Town	County	State	Storm Count	Duration (hours)	Equivalent Days	% of Study Period
A	Amarillo	Potter	TX	56	392.2	16	2.1
E	Channing	Hartley	TX	128	987.8	41	5.2
G	Cheyenne Wells	Cheyenne	CO	119	858.1	36	4.5
I	Clovis	Curry	NM	62	407.7	17	2.1
K	Dalhart	Dallam	TX	122	678.7	28	3.6
M	Guymon	Texas	OK	107	746.5	31	3.9
N	Hereford	Deaf Smith	TX	53	331.0	14	1.7
R	Liberal	Seward	KS	196	1607.7	67	8.5
S	Littlefield	Lamb	TX	91	529.4	22	2.8
T	Memphis	Hall	TX	45	291.7	12	1.5
U	Perryton	Ochiltree	TX	75	488.5	20	2.6
V	Springfield	Baca	CO	139	936.6	39	4.9
X	Stratford	Sherman	TX	123	954.7	40	5.0
Z	Vega	Oldham	TX	59	392.6	16	2.1

Springfield, CO, beginning at 8 a.m. on September 11th, 1939 and lasting through 10 a.m., September 15th. The locations experiencing the greatest ratio of soil damage to event frequency, i.e. where events tended to produce more severe damage per occurrence, are Guymon, OK, Springfield, CO, and Stratford, TX (Fig. 7, sites M, V, and X). These sites and two others (Dalhart, TX, site K; Liberal, KS, site R) within the area of persistent, severe eolian erosion designated by the SCS were situated in counties with, on average, ˜48% of land under cultivation by 1935 and ˜25% coverage by eolian deposits.

The typical Dust Bowl dust event, as defined by the median parameter value on Southern High Plains dust event days (DEDs; Fig. 6b), began between 8 and 11 AM (>40% of all events), lasted eight hours, and originated in counties with ˜50% area under cultivation and 16% coverage of antecedent eolian deposits. The average maximum 2-m windspeed associated with an event causing slight soil damage was ˜9 m s^{-1}, moderate damage occurred with winds an average of 10.9 m s^{-1}, and severe damage with a mean velocity of 18 m s^{-1}. Daily surface air temperatures on a median DED reached a maximum of 19.4°C, with a mean of 11.1°C, and coeval precipitation levels were at a 30% deficit with the most recent rainfall six days prior to the dust event. Median atmospheric conditions on DEDs exhibited temperatures ˜15°C at 850 hPa, with geopotential heights (GPH; defined as the height above sea level of a pressure level) ranging from 110 m at 1000 hPa to 12,133 m at 200 hPa, and potential evapotranspiration (PET) rates of 295 W m^{-2}. Median DED relative humidity was 53%, estimated soil moisture content was 501 kg m^{-2}, atmospheric water vapor content (PWAT) was 19.6 kg m^{-2}, and the energy flux of direct evaporation from bare soil (EVBS) occurred at 32 W m^{-2}. Pairwise correlation analysis indicates that there is significant dependence between climatic conditions on DEDs,

though few variable pairs received an R_S above the threshold indicative of strong monotonic correspondence. PET trends positively with air temperature at 850 hPa (R_S = 0.865, p-value <0.01). In turn, lower-level atmospheric temperature shares a positive correlation with GPH at 500 and 200 hPa (R_S = 0.859 and 0.885 respectively, p-value <0.01). Also related to the availability of water, the relationship between specific humidity at the surface is strongly monotonic with PWAT (R_S = 0.905, p-value <0.01). Of note is the robust relation between the surface (2-m) air temperature retrieved from the Global Historical Climate Network and the 20th Century Reanalysis datasets, indicating strong agreement between the observed historical temperature data and modeled reanalysis data.

3.1. Principal components of dust event days on the Southern High Plains, April 1938 to May 1940

Dust event days can be characterized by six principal components (PCs) that each account for ≥5% of the variance, in total capturing >60% of the variance of all observations (Fig. 8a). Seventeen PCs explain 90% of the variance, though the additional 11 PCs contribute individually ≤4% and are of questionable significance for the characterization of Dust Bowl dust events. A triplot of the first three PCs reveals a gradient in observations and covariances between included variables (Fig. 8b). At the landscape level, changes to visibility and extent of soil damage appear to covary with the proportion of land under cultivation in the county of dust event origin. Dust event seasonal occurrence covaries with the extent of eolian deposits and number of days since the most recent precipitation. The first PC explains 18.5% of the variance and is
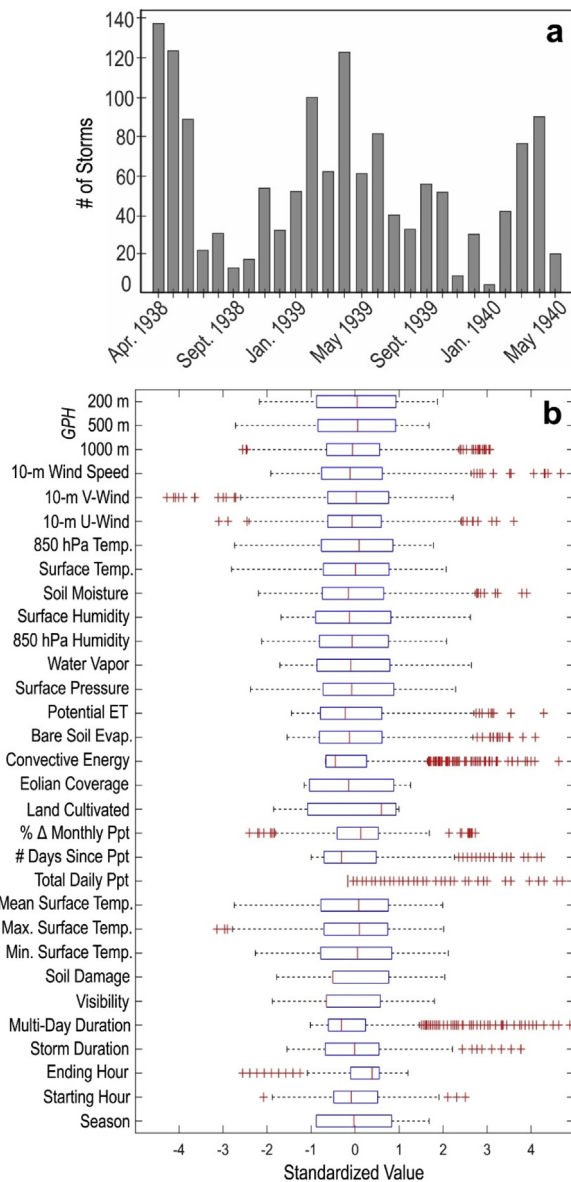
Fig. 6. (a) The total number of dust events recorded each month across the 14 experiment sites between April 1938 and May 1940, inclusive. (b) A boxplot of documented event characteristics and interpolated meteorological and atmospheric conditions on dust event days, with the distribution of each variable standardized by mean and standard deviation.
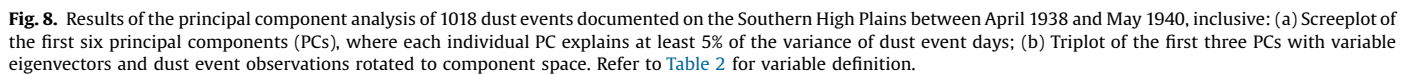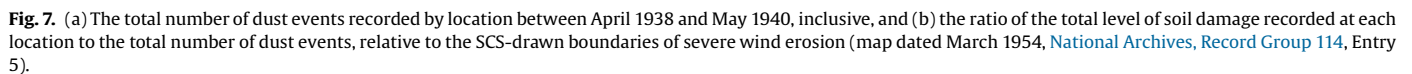
positively correlated to air temperature at 850 hPa, which covaries with GPH at 200 and 500 hPa, and PET; conversely, the second PC is positively correlated with observed mean surface air temperature on DEDs and explains 14% of the variance. The third PC captures 8.2% of variance and is predominantly associated with relative humidity at 850 hPa. This atmospheric moisture metric covaries with soil moisture levels and PWAT, and the strength of meridional winds. The fourth PC explains 7.2% of the variance and is related to the total duration of dust events, which is correlated to EVBS and the hour of day a dust event began. A gradation in dust event intensity is reflected by the fifth PC, elucidating 6% of variability and associated with the occurrence of multi-day events, increasing levels of soil damage, and decreasing visibility. Finally, 5.2% of the variance is explained by the sixth PC, related to the percent coverage of eolian deposits in the county of event origin, covarying with higher windspeeds, lower soil moisture, and near-surface GPH at 1000 hPa.

3.2. Linkages between dust events and covariance with meteorological conditions

Hierarchical clustering analysis yields categorization of dust events into four broad clusters based on the distance between observations in component space (Fig. 9). Euclidean distance and cosine distance measures return the strongest cophenetic correlations of 0.689 and 0.556, respectively. Though clustering analysis using Euclidean distance measures a stronger cluster tree, this linkage differentiates only twelve dust events from other observations: ten events that occurred with cooler air temperatures than other Southern High Plains dust events (Fig. 9b, cluster 4), and the two events most positively correlated with PC 1 (Fig. 9b, cluster 3) and PC 2 (Fig. 9b, cluster 1). Cosine distance, however, distinguishes event clusters based on the relative contribution of the first three PCs, corresponding to air temperature at 850 hPa and surface levels, and relative humidity at 850 hPa (Fig. 9d).

The smallest cosine-distance cluster (1, Fig. 9d) consists of 40 events occurring irrespective of season, when surface air temperatures were virtually equal to temperatures at 850 hPa, such as which occurs near the center of a low-pressure area. These events were most often documented in the Texas panhandle near the cities of Amarillo (A), Stratford (X), and Vega (Z), typically coeval with the highest soil moisture levels and EVBS rates of all dust-event days, occurring ≤5 days since rainfall, with the lowest surface pressures and GPH at 1000 hPa. Clusters 2 and 3 apparently discriminate between early and late "blowing season" (MAMJJA) dust events. The hundreds (420) of dust events within cluster 3 often occur in March and April, when temperatures at 850 hPa are ~10°C warmer than at the surface and relative humidity is ~45%. These early spring events are associated with greater surficial PET, PWAT, and specific humidity. Cluster 2 dust events (411) occur in the summer (JJA), concordant with the hottest surface air temperatures at least 10°C higher than other clusters and maxima in convective potential energy. Relative humidity at 850 hPa was typically greater during cluster 2 DEDs, but median levels of PET and PWAT were lower than in any other cluster. Finally, cluster 4 contains 147 observations associated with winter events (DJF). These DEDs are correlated with wetter-than-average months and lower mean surface temperatures than other seasons, but typically occur after extended dry periods (up to 13 days) and with a thermal inversion, similar to spring events.

The PCA indicates that the thermal gradient between the surface and 850 hPa accounts for the majority of the variance in dust events, i.e. the lower atmospheric lapse rate. Broad-scale weakening of the lapse rate occurs over the Southern High Plains (Fig. 10) with air warming as it rises, and this effect is pronounced on spring and winter DEDs by nearly 2 °C compared to days without dust events. Comparable anomalies in relative humidity (PC 3) on spring and winter DEDs are ~10% less than on days with no reported dust events (Fig. 11). Also on spring and winter DEDs, surface windspeeds are ~1-3 m s^{-1} faster than on days without dust events. Summer DEDs exhibit slightly faster surface windspeeds (0.5 m s^{-1}) than on days without appreciable particle emissions, but this is less pronounced than event days in other seasons. All dust event days display weak vertical wind shear between the surface and 850 hPa. Geopotential heights at 1000 hPa on spring DEDs is ~13 m higher than non-event days, contrasted to summer and winter DEDs, when GPH is ~3 m lower than non-event days (Fig. 12). Mean surface wind direction on spring DEDs is 162°, a markedly stronger southeasterly component compared to spring days without dust events. Southerly winds are most common on summer DEDs, and southwesterly winds more pronounced on winter DEDs versus southeasterly winds that typically occur on winter days without dust events.

Fig. 7. (a) The total number of dust events recorded by location between April 1938 and May 1940, inclusive, and (b) the ratio of the total level of soil damage recorded at each location to the total number of dust events, relative to the SCS-drawn boundaries of severe wind erosion (map dated March 1954, National Archives, Record Group 114, Entry 5).

Fig. 8. Results of the principal component analysis of 1018 dust events documented on the Southern High Plains between April 1938 and May 1940, inclusive: (a) Screeplot of the first six principal components (PCs), where each individual PC explains at least 5% of the variance of dust event days; (b) Triplot of the first three PCs with variable eigenvectors and dust event observations rotated to component space. Refer to Table 2 for variable definition.

3.3. Particulate matter flux from Southern High Plains soils

The range of soil textures on the Southern High Plains, from silt-loam to sand, exhibit extensive heterogeneity in particle (PM_{10}) emissivity (Table 5). The dust emissivity estimated from PI-SWERL tests of varying soil surfaces usually increases exponentially above a threshold windspeed ($8–10\,m\,s^{-1}$), dependent on the presence of surface crust and/or soil clods (Fig. 13). This aligns with reported windspeeds between 6 and $14\,m\,s^{-1}$ during dust events in Goodwell, OK in 1937 and 1938 (Table 1) and for dust events inventoried in this study. Disturbed silt-loam and disturbed loam soils, and undisturbed, loose loamy-sand soils emit PM_{10} at a mean rate in the upper quartile of all measured soil emissivity. In contrast, crusted silt loam soils with clods, crusted loam soils, and crusted sandy loam soils exhibit PM_{10} flux rates in the lower quartile of potential emissivity.

The PM_{10} emission rates for a range of windspeeds from disturbed surfaces is significantly fit by a quadratic polynomial function (Fig. 13a, d, e, g), as are rates for loose, sandy soils (Fig. 13i–k). Alternatively, crusted surfaces and those with enhanced surface roughness, such as fluvial sands with gravel or cultivated fields with large soil clods, respond to increasing windspeeds in an exponential function (Fig. 13b,

c, h, l). Disturbed silt-loam soils initiate dust emissions at a magnitude-higher flux rate than other disturbed soil textures post-exposure to the threshold wind velocity, but nearly all disturbed surfaces emit at magnitude-higher rates than crusted surfaces (0.01 versus $0.001\,mg\,m^{-2}\,s^{-1}$; Fig. 14). The maximum flux rate measured of $24 \pm 6\,mg\,m^{-2}\,s^{-1}$ is also associated with disturbed silt-loam soils, though disturbed loam and disturbed sandy loam soils initiate PM_{10} emissivity at a higher level than other surfaces (Table 5). However, the surface roughness introduced by cultivation of silt loam with large clods significantly reduces the potential emissions (Fig. 14b). Interestingly, PM_{10} flux from loose, uncrusted sandy soils formed on dune sands or sandsheet deposits is of the same magnitude as disturbed surfaces with appreciable silt content under equivalent windspeeds (e.g. Fig. 14d–f). A case study of the Dalhart Sand Dune Area in Dallam County, TX, estimates potential dust emissions (PDE) from bare areas over 3.5 km² based on soil texture, land use, and PI-SWERL dust fluxes (Table 5) for a dust storm observed on April 7, 1937. The storm lasted six hours with a wind velocity of $10.3\,m\,s^{-1}$ causing moderate soil damage. Loamy sand soils that contain appreciable dust-sized particles produced some of the largest volumes of dust, compared to sand dunes or variably crusted sandy loam soils. Subsoils (likely B-horizons) emitted at similar rates compared to sandy loam soils. Dust emission is
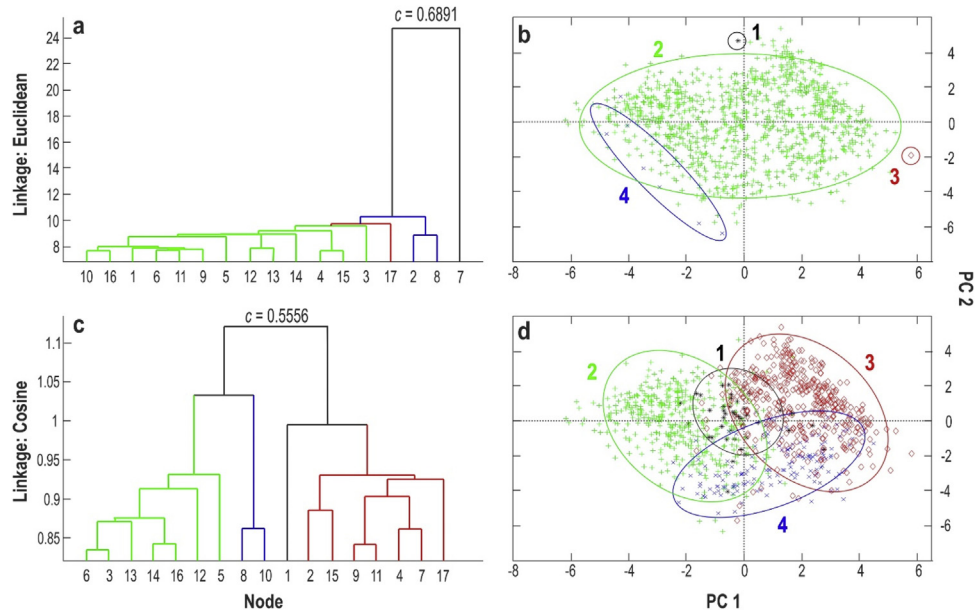
Fig. 9. Hierarchical cluster trees and distribution of dust event clusters in principal component (PC) space: (a, b) Euclidean distance, and (c, d) Cosine distance, with cophenetic correlation coefficient (*c*).
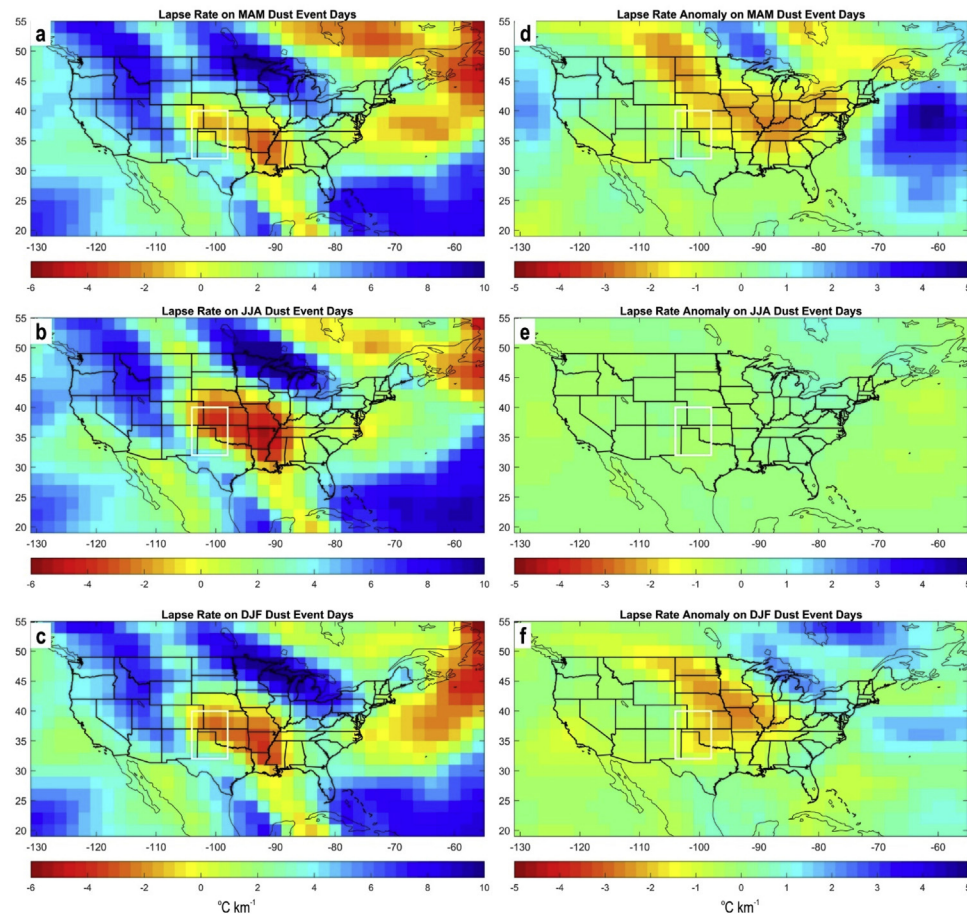
Fig. 10. (a–c) Lapse rates between the surface and 850 hPa pressure level on dust event days between April 1938 and May 1940, and (d–f) lapse rate anomalies on dust event days calculated against mean lapse rates on days without dust events in the same season for: spring (MAM, top row), summer (JJA, middle row), and winter (DJF, bottom row). White box demarcates the Southern High Plains region. Calculated using the 20th Century Reanalysis Project, V2c (Compo et al., 2011).
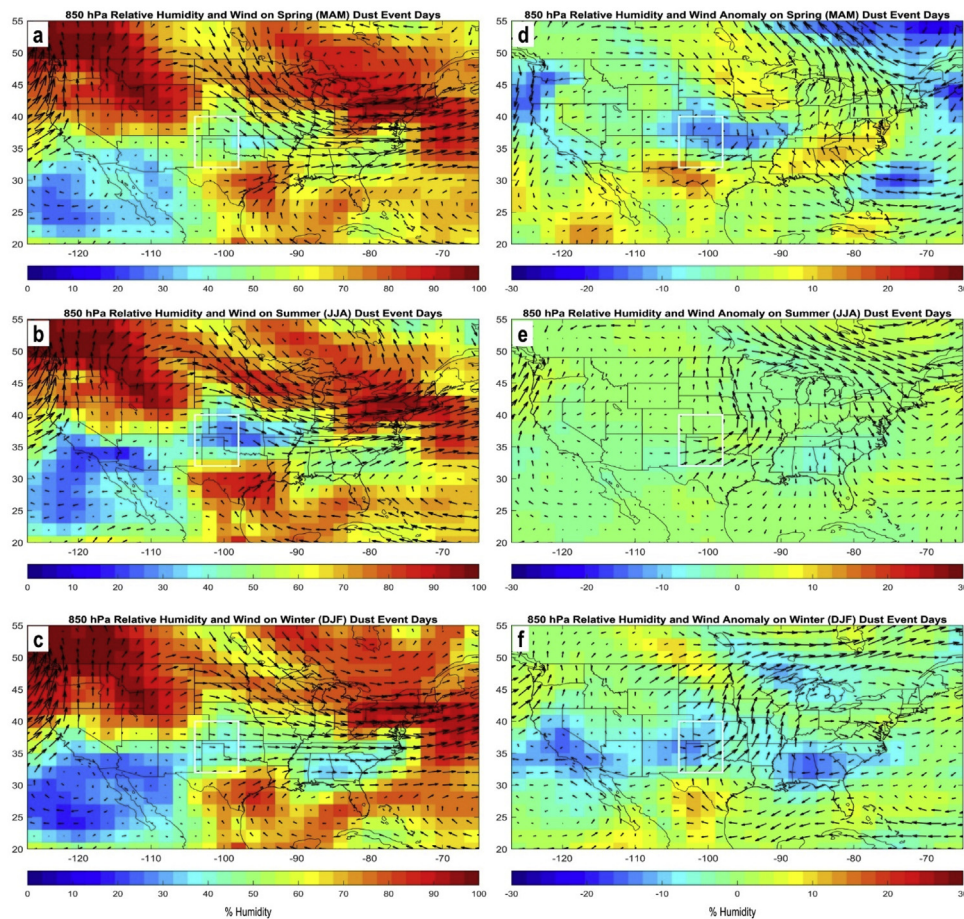
Fig. 11. Same as Fig. 10, but for relative humidity and winds at 850 hPa pressure level.

largely driven by saltation bombardment and the release of fines in this setting. We estimate that ˜112 to 569 kg PM_{10} could have potentially been emitted from the bare soil surfaces considered based on the derived flux curves (Fig. 15).

4. Discussion

4.1. Controls on dust event variability at the heart of the Dust Bowl

The parallel gradient between windspeed and degree of soil movement during dust events emulates the reported co-occurrence of increasing wind velocities with increasing volumes of dust deposition and decreasing visibility in other historical records (cf. Table 1). This is also consistent with observations from the Dalhart experiment station that noted dust events often occurred with windspeeds > 8.9 m s^{-1} (National Archives, Record Group 114, Entry 112). The frequency of dust events during the Dust Bowl was equivalent to or greater than events in dry land areas in present-day northern China (Qian et al., 2004), Mongolia (Natsagdorj et al., 2003), North Africa (Mallone et al., 2011; Gkikas et al., 2013; Stafoggia et al., 2016) and the desert U.S. Southwest (e.g. Flagg et al., 2014; Eagar et al., 2017). In the core wind erosion area of the Oklahoma and Texas panhandles, and adjacent areas in Kansas and Colorado, up to 140 dust episodes per year were recorded between 1936 and 1940. The highest-magnitude dust event in the period considered here is nearly twice as long in duration as dust storms recorded at Lubbock, TX between 1947 and 1989 (Lee and Tchakerian, 1995). The PCA analysis highlights the impact of elevated temperatures and reduced relative humidity at 850 hPa

(i.e. a weakened Great Plains Low Level Jet; GPLLJ) in propagating dust activity in the 1930s (Donat et al., 2016; Cowan et al., 2017; Hegerl et al., 2018). The covariance between temperature at 850 hPa and geopotential heights at 500 and 200 hPa is consistent with documented extraordinary summer heat that likely exacerbated land-surface feedbacks associated with subsequent spring aridity (Donat et al., 2016; Cowan et al., 2017), and would enhance atmospheric subsidence, warming the lower troposphere and increasing near-surface windspeeds (Cowan et al., 2017; Pu and Ginoux, 2018).

Intense drought and extreme temperatures further contributed to reduction in vegetation cover (McDowell, 2011), making previously-stabilized surfaces susceptible to eolian erosion (Albertson and Weaver, 1944) and increasing surface albedo (Schlesinger et al., 1990). The influence of temperature and relative humidity on the strength of DBD dust events is consistent with inferred processes in fine dust generation for the western U.S., which find that atmospheric dust concentrations depend on temperature-related feedbacks to synoptic transport (Tai et al., 2012; Achakulwisut et al., 2017). The PCA also demonstrates the elevated temperatures intensified evaporation from bare soil surfaces (EVBS), depleting soil moisture reserves in late spring and summer (Lee and Gill, 2015), which has been shown to autocorrelate with precipitation anomalies in the subsequent spring (Nandintsetseg and Shinoda, 2015). This indicates that a number of meteorological factors were necessary, beyond those simulated by the PI-SWERL, to set up the conditions for enhanced long-term wind erosion and dust transport over a large area that typified the Dust Bowl.
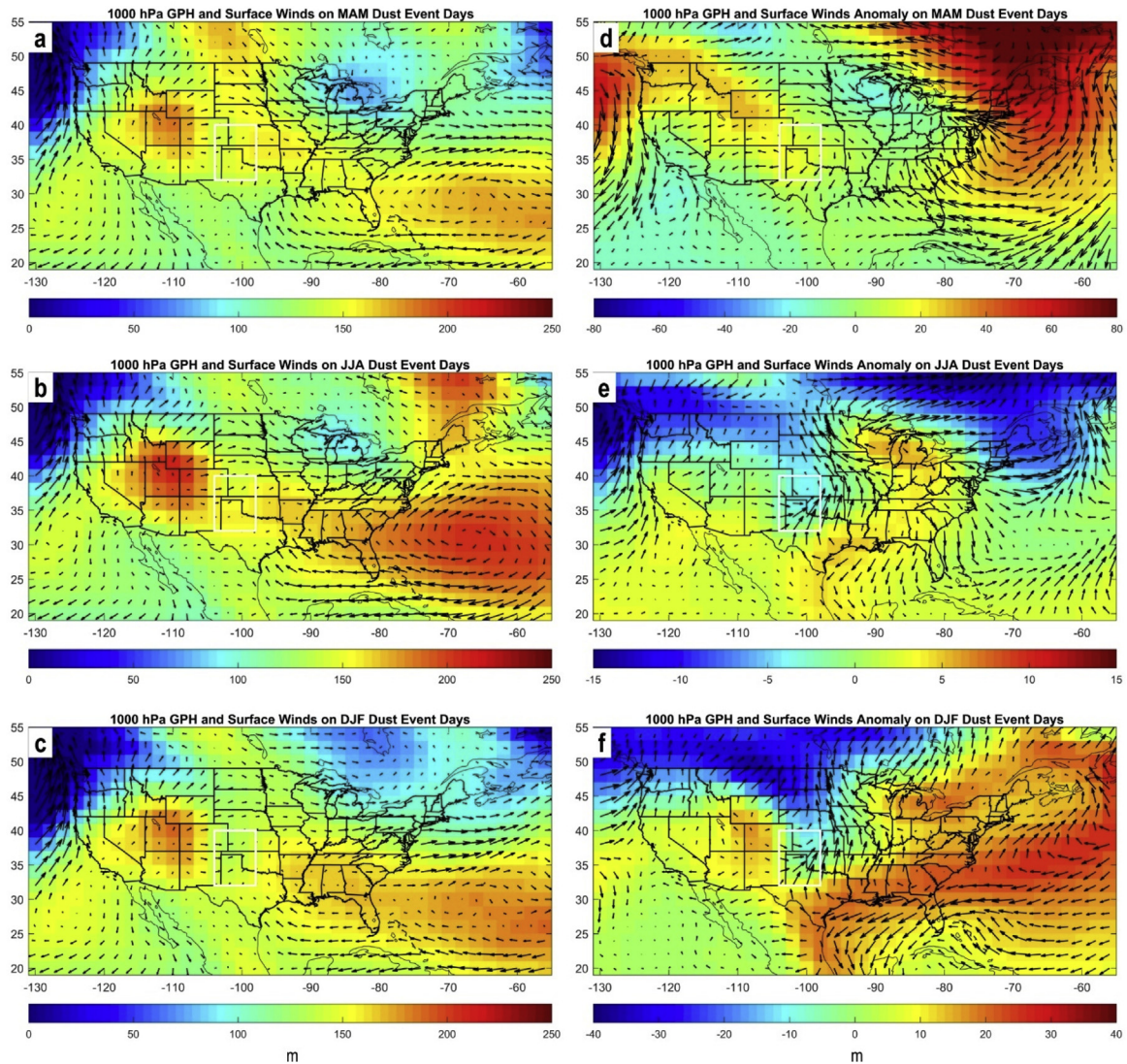
Fig. 12. Same as Fig. 10, but for geopotential heights (GPH) at 1000 hPa pressure level and surface winds.

Table 5
Descriptive statistics of particulate matter (PM_{10}) flux values measured by the PI-SWERL for each surface soil condition and selected regression to predict PM_{10} flux, with root mean squared error (RMSE) and for linear models the adjusted R^2, where the given wind speed (x) is first normalized to the mean (μ) and standard deviation (σ) of the range of tested wind velocities.

Plot	Soil Condition	Sample Density	PM_{10} Flux (mg m^{-2} s^{-1})				Function	RMSE (mg m^{-2} s^{-1})	Adj. R^2	Wind Speed (m s^{-1})	
			Minimum	Maximum	Average	STD				μ	σ
a	Disturbed Silt Loam	54	0.002	23.941	4.955	5.832	$f(x) = 0.511x^2 + 3.455x + 3.797$	3.683	0.601	21.12	6.392
	Crusted Silt Loam	69	0.003	17.363	1.515	3.348	$f(x) = 0.108^{2.397x}$	0.609	—	14.41	4.091
b	Disturbed Silt Loam w/ Clods	26	0.002	3.223	0.575	1.006	$f(x) = 0.086^{0.886x}$	0.359	—	21.9	7.76
	Crusted Silt Loam w/ Clods	19	0.007	1.900	0.368	0.474	$f(x) = 0.19^{0.627x}$	0.205	—	18.93	6.385
c	Disturbed Loam	22	0.014	13.816	3.657	4.416	$f(x) = 1.169x^2 + 3.563x + 2.598$	2.149	0.763	17.4	6.001
	Crusted Loam	20	0.007	2.214	0.384	0.674	$f(x) = 0.2864^{0.894x}$	0.585	—	14.68	4.299
d	Disturbed Sandy Loam	42	0.011	13.816	2.026	2.596	$f(x) = 0.815x^2 + 1.882x + 1.267$	0.8276	0.898	17.51	5.495
	Crusted Sandy Loam	16	0.002	0.573	0.095	0.161	$f(x) = 0.025^{1.346x}$	0.024	—	15.18	4.63
	Crusted Sandy Loam Mantled w/ Windblown Sand	90	0.006	13.202	1.922	2.141	$f(x) = 1.247^{0.732x}$	1.05	—	17.51	5.495
e	Loose Loamy Sand	53	0.007	19.722	2.117	2.810	$f(x) = -0.166x^2 + 1.06x + 1.745$	0.893	0.566	16.84	5.031
f	Loose Sand	63	0.002	6.157	1.237	1.296	$f(x) = 0.009x^2 + 0.098x + 0.121$	0.4792	0.863	16.98	4.66
	Loose Sand w/ Gravel	11	0.004	2.772	0.736	1.007	$f(x) = 0.13^{2.237x}$	0.161	—	23.24	6.947
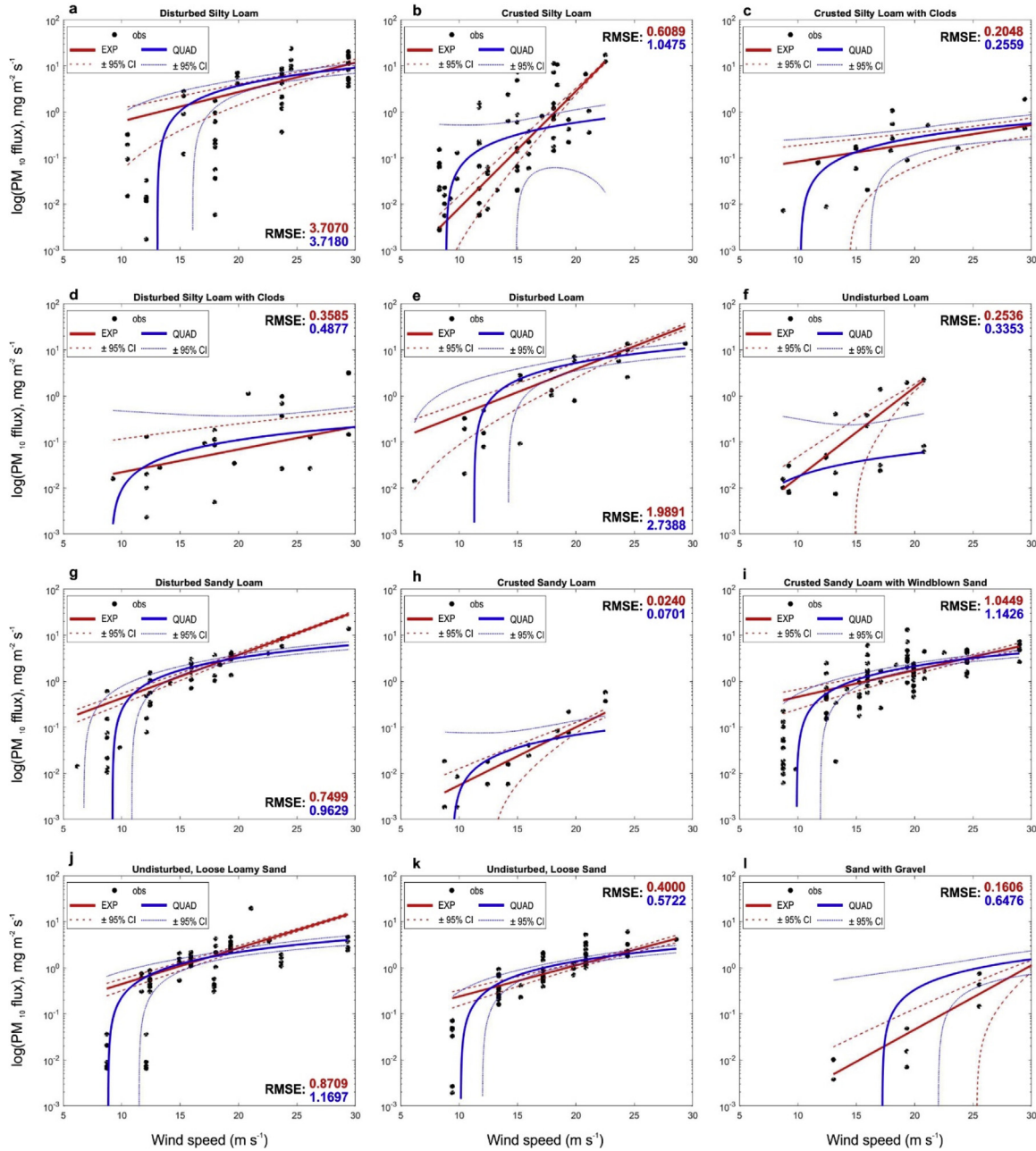
Fig. 13. Comparison of exponential (EXP) and quadratic polynomial (QUAD) models for PI-SWERL particle flux concentration measurements as a function of windspeed, binned by soil texture and surface treatment.

4.2. Four dominant modes of Dust Bowl dust events

The inferred clusters of dust events yield insights on the different synoptic conditions conducive for surface erosion and mesoscale dust transport predominately related to the seasonal cycle, similar to findings of Lee and Tchakerian (1995) and Novlan et al. (2007) among others. The first (second) mode of dust events is connected to enhanced high-pressure anomalies, in tandem with increased agricultural activity, during spring (winter) months. Specifically, an increase in geopotential heights (Fig. 12d, f) and concomitant weakened lapse rate (Fig. 10d, f) on dust event days results in consistent entrainment and concentration of particles in the lower atmosphere. The presence of an anomalous high-pressure outflow in the middle-to-upper troposphere is associated

with a strong negative feedback between soil moisture and precipitation and would suppress convection and generate strong winds (Cook et al., 2011; Su et al., 2014). Though the weakened lapse rate would suppress vertical mixing, it would also increase diurnal surface heating, which encourages transfer of momentum from winds aloft to the surface (Sridhar et al., 2006) and inversion-shear converging dust in the boundary layer (Rendón et al., 2015).

The third mode of dust events occurs with a peak in surface temperatures (>35°C) relative to temperatures at 850 hPa in summer (JJA), associated with an increase in the number of dust events beginning in the afternoon. This cluster is typically associated with low potential evapotranspiration, low atmospheric water vapor content and reduced specific humidity, possibly reinforcing drought conditions through increasing surface
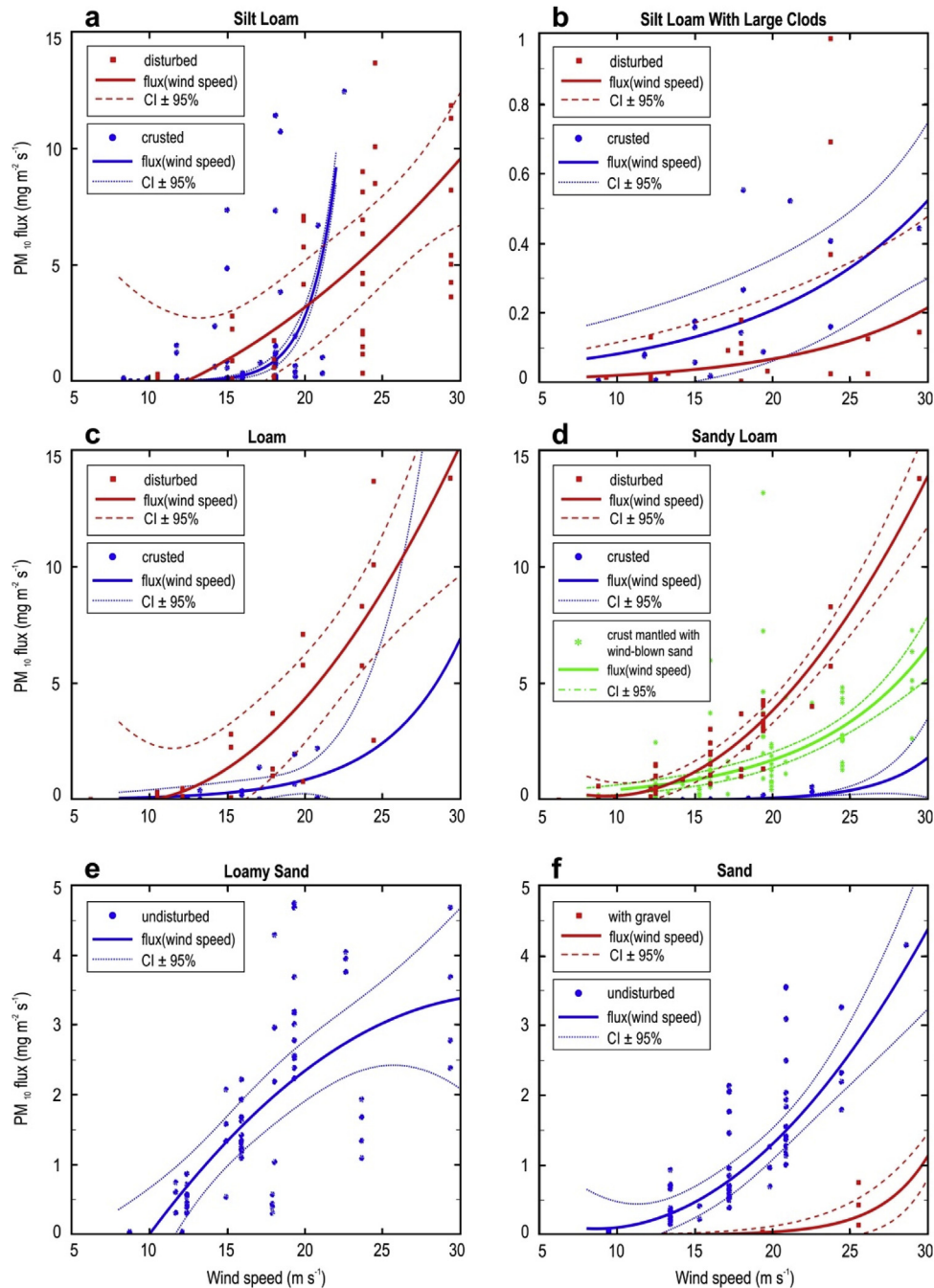
Fig. 14. Selected regressions for each soil texture contrasting response from disturbed, undisturbed, and crusted surfaces, where particulate matter (PM$_{10}$) flux is calculated as a function of normalized wind speeds. Refer to Table 5 for curve formulas and associated goodness-of-fit parameters.

latent-heat flux related to decreasing soil moisture (Hong and Kalnay, 2000; Xu et al., 2004) and through diminished net primary productivity (Hong and Kalnay, 2000; Nandintsetseg and Shinoda, 2015). Summer dust event days display weak anomalies in lapse rates (Fig. 10e), relative humidity (Fig. 11e) and surface geopotential heights (Fig. 12e). This suggests that land surface conditions become more significant in explaining the occurrence of summer dust events, related to diurnal surface heating from dry, bare soil surfaces. These dust events often occur with southerly and southwesterly winds and generate extensive soil erosion, associated with peak surface windspeeds (>10 m s^{-1}), and very high dust concentrations (Table 1). Weak vertical wind shear during JJA dust events will isolate updrafts from the low-level moisture supply, i.e. the GPLLJ, which was broadly weakened during the 1930s (Donat

et al., 2016), but exerts the strongest presence in this season (Fig. 11b). This allows for more frequent dry, hot southwesterly winds across the Great Plains from Mexico and the southwest U.S. during these summer months (Fig. 12d; Schmeisser et al., 2010).

The fourth dust event mode discriminates cold-frontal haboobs (Lee and Gill, 2015), forming irrespective of season and dominantly occurring over the Texas panhandle with a uniform thermal gradient from the surface to 850 hPa, which is consistent with the passage of a cyclone (Warn, 1952; Lee and Tchakerian, 1995; Rivera Rivera et al., 2009). When these events occur, there are low levels of atmospheric water vapor, but soil moisture content and direct evaporation from bare soil surfaces are 25 to 70% higher than during other modes. The low GPH at 1000 hPa and deep convection indicated by the increased rates of direct evaporation further
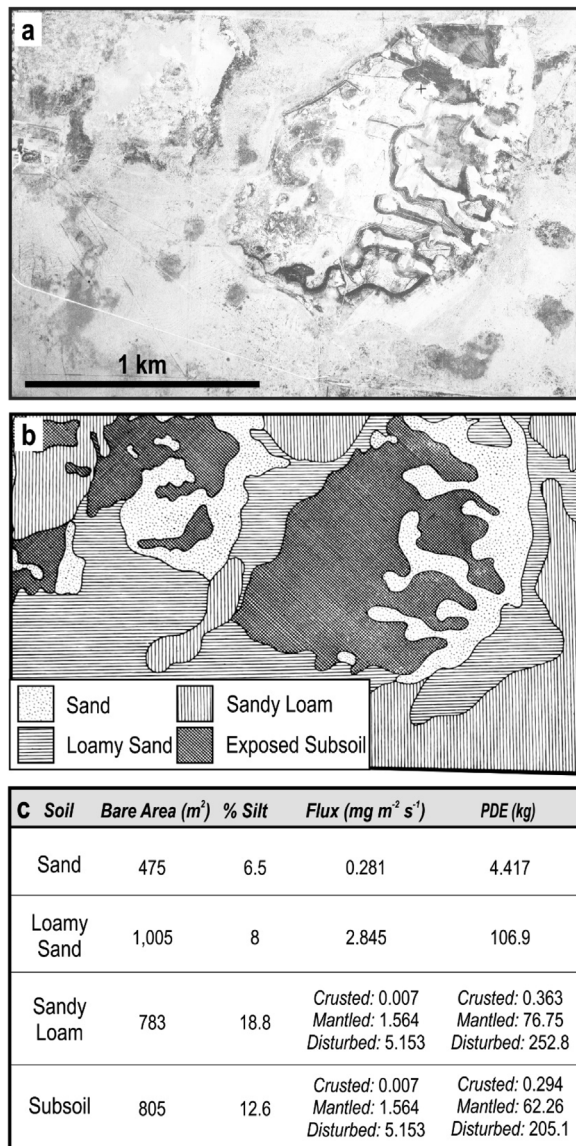
Fig. 15. Potential dust emissions (PDE) from the Dalhart Sand Dune Area in Dallam County, TX for a event observed on April 7, 1937. (a) Aerial photograph of the case-study area captured on October 5, 1936 (National Archives, Record Group 114, Frame AG-137-55). (b) Contemporaneous soil texture map produced by the Soil Conservation Service (Eby and Whitfield, 1940). (c) Available bare surface area in photograph to emit dust by soil texture, the percent silt in the mapped soil unit, the derived PM$_{10}$ flux rate from equations in Table 5, and inferred PDE.

(Williams, 2007; Sow et al., 2011; Yair et al., 2016). Many dust events during the Dust Bowl and earlier droughts were associated with substantial free-electrical discharges that charred telephone poles, stranded cars, and disrupted power service (e.g. Hovde, 1934; Choun, 1936). Particle collision with particularly low humidity conditions induces formation of a static electric charge, restricted usually to ̃1 km above the surface (Nicoll et al., 2011; Sow et al., 2011; Yair et al., 2016). Thus, the tribocharging of sand grains was a potential factor for intensification of dust events leading to exceptionally low visibility (<10 m) during the Dust Bowl, like conditions on the infamous Black Sunday, on April 14, 1935 (Fig. 2c; Stallings, 2001).

The ubiquity of 1930s dust events is often attributed to the use of unsuitable lands for cultivation (cf. Bennett and Fowler, 1936; Johnson, 1947; Worster, 1979; Hurt, 1981; Hansen and Libecap, 2004). The principal components of dust events indicate that only 2.6% of variance of observed dust events is attributed to the extent of land under cultivation by 1935. This would suggest that the persistence of dust events was not exclusively related to poor agricultural stewardship but also influenced by the desiccation of sandy lands left as range (Albertson and Weaver, 1942, 1944), which accounts for >5% of the variance of dust-event days. Indeed, sand dunes are developed on many areas throughout the Great Plains, particularly between the Arkansas and Canadian rivers within the specified area of severe wind erosion (Fig. 7; Whitfield, 1938; Forman et al., 2001, 2008). However, this influence changes seasonally, with the timing of cultivation significant during spring and winter dust events, in keeping with Lee and Tchakerian's (1995) study of dust events on the Southern High Plains since 1947. In contrast, the influence of exposed eolian deposits in rangelands is apparently more significant than meteorological anomalies for summer dust events, likely related to elevated temperatures exacerbating soil moisture deficits and inhibiting development of soil crusts strong enough to dampen eolian erosion on surfaces with high sand content.

4.3. Short-term potency versus long-term cumulative particle emission from Southern High Plains soils

The PM$_{10}$ dust fluxes measured by PI-SWERL in this study are similar to those measured from eolian sands in the Mojave Desert and China (Sweeney et al., 2011, 2016a), and crusted and disturbed loess in Nebraska (Sweeney and Mason, 2013). A broader assessment of the still and aerial photographic record and primary documentation from Soil Conservation Service (SCS) experiment stations reveal a range of land surface conditions from fully vegetated to eolian-eroded, denuded surfaces during the DBD. This complex landscape mosaic is consistent with concepts of heterogeneous ecosystem response to extreme drying or precipitation variability (cf. Schlesinger et al., 1990; Peters et al., 2015; Gherardi and Sala, 2015). Twenty-first century dust events in the southern U.S. exhibit similar characteristics and are often point-sourced to cropland or rangeland on the Southern High Plains (e.g. Lee et al., 2009). PI-SWERL tests reveal that disturbed soils in this region begin to emit at a magnitude-higher rate than undisturbed surfaces when the threshold wind velocity (8 to 10 m s^{-1}) is met, and this rate increases linearly with windspeed. Conversely, crusted, undisturbed surfaces do not begin to reach the same flux rate until much higher windspeeds, at which point the crusts are broken and emissivity rates increase rapidly, similar to disturbed surfaces. These higher threshold velocities also are common to variably crusted and clodded cultivated soils (Gillette, 1988). Loamy sand and sandy loam soils are particularly potent emitters when compared to other soil textures

suggest the presence of a steep, low-pressure front (Sidwell, 1938; Smith et al., 1970; Idso et al., 1972; Chen and Fryrear, 2002; Novlan et al., 2007), and correlate with events that began earlier in the day, persisted for ≥24 h, and with visibility <10 km. The frequency of haboobs over panhandle counties suggests greatly diminished primary productivity to enable such increases in evaporation from soil surfaces on any given day of year. However, areas associated with this mode were neither heavily cultivated, nor with appreciable coverage by eolian deposits, yielding uncertainty on the land use or landforms contributing to dust event generation (Vivoni et al., 2009). Dust events propagated by thunderstorms, passing fronts, and/or movement of low-pressure systems often transport dense concentrations of suspended particles (Table 1; >1 g m^{-3}) and can be associated with a magnitude increase in electrostatic charge from saltating sand and Brownian motion of suspended particles, which is an underappreciated natural hazard

(Fig. 15c), which is supported by numerous studies (Gillette, 1979; Gillette et al., 1988; Nickling and Gillies, 1989). In the Southern High Plains, Lee et al. (2009) identified sandy loam soils as a hot spot for dust point sources. In general, sandy soils are some of the most erodible by wind and are key sources of global dust (Bullard et al., 2011; Crouvi et al., 2012). Significantly, the particle emissivity of undisturbed, loose sandy soils mirrors that of disturbed surfaces in relation to windspeed and potential magnitude of dust emitted. This suggests that some bare, sandier, uncultivated soils of the Southern High Plains could be equal to or greater dust sources than cultivated fields during periods of intense aridity causing native vegetation mortality. Cultivated surfaces are seasonally unavailable dust sources either via crop cover or soil crust formation between agricultural treatments. In contrast, dunes and sandsheets persist as available dust sources year-round with the inhibited development of biological surface crusts stemming from extensive vegetation loss (Veste et al., 2001). Furthermore, the higher relief of eolian landforms, combined with the decreased shear velocity from reduced plant cover, increases sand mobility under higher windspeeds (Lancaster, 1985; Wiggs et al., 1994; Veste et al., 2001). These sand grains, if blown into fields from surrounding denuded areas, could pulverize surface crusts similar to the process of particles pitting and frosting automobile windshields during dust events (Disterdick, 1933; Martin, 1938).

Associated Press journalist Robert Geiger, credited with coining the term "Dust Bowl," wrote of the dust as he travelled through Guymon, OK: "It gets into your clothes, literally in your hair, and sometimes it seems in your very soul. Certainly it gets under the skin" (Geiger, 1935). The anomalously elevated temperatures during the 1930s (Donat et al., 2016; Cowan et al., 2017) account for one-third of the variability in Dust Bowl dust event activity, which carries significant implications for a warming world (e.g. Cook et al., 2015). Dust sources on the Southern High Plains abound with predominately sandy soils and are often associated with antecedent dunes and cover sands. Climate models forecast significant aridity and decade-long droughts on the Great Plains for later in the 21st century coincident with extreme, elevated summer temperatures (Woodhouse et al., 2010; Cook et al., 2015), ideal conditions for vegetation mortality and formation of haboobs, the quintessential characteristics of the DBD. Such continental-scale dust events would increase PM loads >20 μg m^{-3} d^{-1}, would be detrimental for public health in nearby urban centers (Tong et al., 2017), and potentially across North America, dependent on synoptic conditions. Shortgrass prairie in the driest areas of the USGP may shift in ecosystem function with an increase in surficial heterogeneity, like those of the desert grasslands in the SW (Schlesinger et al., 1990; Mangan et al., 2004; Collins et al., 2014; Moran et al., 2014; Svejcar et al., 2015) and similar to landscape response in the 1930s (Bolles and Forman, 2018). Like during the Medieval Climate Anomaly megadroughts (Woodhouse and Overpeck, 1998; Forman et al., 2001; Miao et al., 2007; Stahle et al., 2007; Cook et al., 2010; Hanson et al., 2010; Woodhouse et al., 2010), this could potentially precipitate a magnitude increase in mineral dust aerosol emissions from the Southern High Plains.

5. Conclusion

The Dust Bowl of the 1930s was an iconic event of environmental degradation across the U.S. Great Plains with crop failure, denudation of uncultivated and cultivated lands, and with numerous loci for the generation of fugitive dust. This study accessed primary historical archives, the Global Historical Climate Network, the 20th Century Reanalysis Project, field surveys and measurements with a Portable In-Situ Wind Erosion Laboratory, to assess the controls and character of dust event variability and soil surface emissivity across the Southern High Plains resulting from persistent and intense periods of aridity. For the first time, a continuous, quantitative and spatially-explicit record of dust events was compiled across the core Dust Bowl region from April 1938 to May 1940, which enabled investigation of three main objectives related to meteorological and land surface conditions. In summary:

(1) Lower-level atmospheric and surface air temperatures are the strongest principal components driving the variance in Dust Bowl dust events, followed by low-level relative humidity. Anomalies in this thermal gradient (i.e. the lapse rate) and moisture carried by the Great Plains Low Level Jet occurred on dust event days that were not present on days without dust events within the same season. The extent of antecedent eolian deposits in the Dust Bowl region explains more variance in dust events than the extent of land under cultivation.

(2) Four modes of dust events were identified related to the season of occurrence and dominant meteorological controls, with land surface conditions a secondary factor. Two modes characterize "blowing season" events, with spring (MAM) dust events related to an inversion of surface and atmospheric air temperatures, and summer (JJA) dust events associated with intensified surface heating. The third mode of dust event occurs during the winter (DJF) after an extended dry period, and the fourth dust event mode reflects the passage of vigorous cold-frontal haboobs occurring irrespective of season. The seasonal timing of agriculture is correlated with the occurrence of spring and winter dust events, whereas the presence of sandier soils and eolian landforms correlate strongly to the occurrence of summer dust events.

(3) Assessment of the potential PM$_{10}$ emissivity from common dust sources across the Southern High Plains indicates that anthropogenic disturbance of surface crusts can increase the magnitude of particle emissions (0.001 to 0.01 mg m^{-2} s^{-1}) from siltier soils. However, emissions from loose, uncultivated sandy soils can emit similarly potent levels of dust as disturbed cultivated surfaces, suggesting a more complex narrative than previously recognized for landscape degradation in the 1930s Dust Bowl.

Declaration of Competing Interest

The authors declare that they have no known competing financial interests or personal relationships that could have appeared to influence the work reported in this paper.

Appendix A. PI-SWERL site locations

PI-SWERL Site	County	Description	Lat(dec. deg)	Lon(dec.deg)
Colorado				
BK1	Baca	Cultivated* loess	37.557024	−102.609578
BSF1	Baca	Sandsheet	37.235736	−102.561183
BSF2	Baca	Dune	37.235934	−102.560986
BSF3	Baca	Cultivated/ sandsheet	37.236075	−102.502132
BTB1	Baca	Cultivated loess	37.473462	−102.364307
BTB2	Baca	Cultivated loess	37.553255	−102.36484
BTB3	Baca	Cultivated loess	37.472949	−102.364264
BV1	Baca	Clutivated fluvial	37.354874	−102.447606
PL1	Prowers	Dune/paleosol	38.042942	−102.617075
Kansas				
HK1	Hamilton	Dune	37.864014	−101.579018
HK2	Hamilton	Cultivated loess	37.856333	−101.579142
HK3	Hamilton	Cultivated loess	37.832904	−101.578927
HK4	Hamilton	Cultivated loess	37.827375	−101.579057
HS1	Hamilton	Dune	37.960003	−101.754956
HS2	Hamilton	Dune/paleosol	37.959783	−101.759321
HS3	Hamilton	Fluvial terrace	37.965296	−101.756456
HS4	Hamilton	Fluvial terrace	37.96406	−101.755241
KL1	Kearny	Cultivated loess	37.929567	−101.361552
Oklahoma				
BB1	Beaver	Cultivated fluvial	36.868117	−100.656893
BB2	Beaver	Dune	36.828912	−100.701956
BB3	Beaver	Fluvial terrace	36.765142	−100.613525
BB4	Beaver	Dune/paleosol	36.83667	−100.516285
BBA1	Beaver	Cultivated fluvial	36.654741	−100.684458
BBA2	Beaver	Cultivated loess	36.659829	−100.658074
BBA3	Beaver	Cultivated loess	36.659939	−100.63702
BF1	Beaver	Sandsheet	36.881228	−100.585245
BT1	Beaver	Fluvial terrace	36.735492	−100.792574
Texas				
DD1	Dallam	Cultivated/subsoil	36.15072	−102.627065
DD2	Dallam	Sandsheet	36.194328	−102.629377
DD3	Dallam	Dune	36.154042	−102.536887
DD4	Dallam	Cultivated/dune	36.15412	−102.540383
DP1	Dallam	Sandsheet	36.271846	−102.796646
DP2	Dallam	Cultivated/subsoil	36.456026	−102.650903

* Cultivated indicates currently cultivated or fallow.

References

Achakulwisut, P., Shen, L., Mickley, L.J., 2017. What controls springtime fine dust variability in the Western United States? Investigating the 2002-2015 increase in fine dust in the U.S. southwest: controlling factors of western U.S. Dust. J. Geophys. Res. Atmos. 122 (22) doi:http://dx.doi.org/10.1002/2017JD027208 12,449-12,467.

Albertson, F.W., Weaver, J.E., 1942. History of the native vegetation of western Kansas during seven years of continuous drought. Ecol. Monogr. 12 (1), 23–51.

Albertson, F.W., Weaver, J.E., 1944. Effects of drought, dust, and intensity of grazing on cover and yield of short-grass pastures. Ecol. Monogr. 14 (1), 1–29.

Bacon, S.N., McDonald, E.V., Amit, R., Enzel, Y., Crouvi, O., 2011. Total suspended particulate matter emissions at high friction velocities from desert landforms. J. Geophys. Res. 116, F03019 doi:http://dx.doi.org/10.1029/2011JF001965.

Baddock, M.C., Ginoux, P., Bullard, J.E., Gill, T.E., 2016. Do MODIS-defined dust sources have a geomorphological signature? Geophys. Res. Lett. 43 (6), 2606–2613. doi:http://dx.doi.org/10.1002/2015GL067327.

Basara, J.B., Maybourn, J.N., Peirano, C.M., Tate, J.E., Brown, P.J., Hoey, J.D., Smith, B.R., 2013. Drought and associated impacts in the Great Plains of the United States—a review. Int. J. Geosci. 04 (06), 72–81. doi:http://dx.doi.org/10.4236/ijg.2013.46A2009.

Bennett, H.H., Fowler, F.H., 1936. Report of the Great Plains Drought Area Committee. Government Printing Office, Washington, DC.

Bolles, K.C., Forman, S.L., 2018. Evaluating landscape degradation along climatic gradients during the 1930s dust bowl drought from panchromatic historical aerial photographs, United States Great Plains. Front. Earth Sci. 6 doi:http://dx.doi.org/10.3389/feart.2018.00153.

Bolles, K.C., Forman, S.L., Sweeney, M., 2017. Eolian processes and heterogeneous dust emissivity during the 1930s Dust Bowl Drought and implications for projected 21st-century megadroughts. Holocene 0959683617702235.

Bochert, J.R., 1971. The dust bowl in the 1970s. Ann. Assoc. Am. Geogr. 61, 1–22.

Borradaile, G., 2003. Correlation and comparison of variables. Statistics of Earth Science Data. Springer, Berlin, Heidelberg, pp. 157–185.

Boucher, O., Randall, D., Artaxo, P., Bretherton, C., Feingold, G., Forster, P., et al., 2013. Clouds and aerosols. In climate change 2013: the physical science basis. Contribution of Working Group I to the Fifth Assessment Report of the Intergovernmental Panel on Climate Change. Cambridge University Press, pp. 571–657.

Brown, E.G., Gottlieb, S., Laybourn, R.L., 1935. Dust storms and their possible effect on health. Public Health Rep 50, 1369–1383.

Brown, M.J., Krauss, R.K., Smith, R.M., 1968. Dust deposition and weather. Weatherwise 21, 66–70.

Bullard, J.E., White, K., 2005. Dust production and the release of iron oxides resulting from the aeolian abrasion of natural dune sands. Earth Surf. Process. Landf. 30 (1), 95–106. doi:http://dx.doi.org/10.1002/esp.1148.

Bullard, J.E., Harrison, S.P., Baddock, M.C., Drake, N., Gill, T.E., McTainsh, G., Sun, Y., 2011. Preferential dust sources: a geomorphological classification designed for use in global dust-cycle models. J. Geophys. Res. 116, F04034 doi:http://dx.doi.org/10.1029/2011JF002061.

Burnette, D.J., Stahle, D.W., 2013. Historical perspective on the dust bowl drought in the central United States. Clim. Change 116, 479–494.

Burnette, D.J., Stahle, D.W., Mock, C.J., 2010. Daily-mean temperature reconstructed for kansas from early instrumental and modern observations. J. Climate 23, 1308–1333.

Camino, C., Cuevas, E., Basart, S., Alonso-Perez, S., Baldasano, J.M., Terradellas, E., Marticorena, B., Rodriguez, S., Berjon, A., 2015. An empirical equation to estimate mineral dust concentrations from visibility observations in Northern Africa. Aeolian Res. 16, 55–68.

Chen, W., Fryrear, D.W., 2002. Sedimentary characteristics of a haboob dust storm. Atmo. Res. 61, 75–85.

Chepil, W.S., 1957. Dust bowl: causes and effects. J. Soil Water Conserv. 12, 108–111.

Chepil, W.S., Siddoway, F.H., Armbrust, D., 1963. Climatic index of wind erosion conditions in the Great Plains. Soil Sci. Soc. Am. J. 27 (4), 449–452.

Choun, H.F., 1936. Dust storms in the southwestern plains area. Mon. Weather Rev. 64, 195.

Collins, S.L., Belnap, J., Grimm, N.B., Rudgers, J.A., Dahm, C.N., D'Odorico, P., et al., 2014. A multiscale, hierarchical model of pulse dynamics in Arid-Land ecosystems. Annu. Rev. Ecol. Evol. Syst. 45 (1), 397–419. doi:http://dx.doi.org/10.1146/annurev-ecolsys-120213-091650.

Compo, G.P., Whitaker, J.S., Sardeshmukh, P.D., Matsui, N., Allan, R.J., Yin, X., Gleason, B.E., Vose, R.S., Rutledge, G., Bessemoulin, P., Brönnimann, S., Brunet, M., Crouthamel, R.I., Grant, A.N., Groisman, P.Y., Jones, P.D., Kruk, M., Kruger, A.C., Marshall, G.J., Maugeri, M., Mok, H.Y., Nordli, Ø., Ross, T.F., Trigo, R.M., Wang, X.L., Woodruff, S.D., Worley, S.J., 2011. The twentieth century reanalysis project. Q. J. R. Meteorol. Soc. 137, 1–28. doi:http://dx.doi.org/10.1002/qj.776.

Cook, B.I., Miller, R.L., Seager, R., 2008. Dust and sea surface temperature forcing of the 1930s "Dust Bowl" drought. Geophys. Res. Lett. 35 (8) doi:http://dx.doi.org/10.1029/2008GL033486.

Cook, B.I., Miller, R.L., Seager, R., 2009. Amplification of the North American "Dust Bowl" drought through human-induced land degradation. Proc. Natl. Acad. Sci. 106 (13), 4997–5001.

Cook, B.I., Seager, R., Miller, R.L., 2011. Atmospheric circulation anomalies during two persistent North American droughts: 1932-1939 and 1948-1957. Clim. Dyn. 36, 2339–2355.

Cook, B.I., Seager, R., Miller, R.L., Mason, J.A., 2013. Intensification of north american megadroughts through surface and dust aerosol forcing. J. Clim. 26 (13), 4414–4430. doi:http://dx.doi.org/10.1175/JCLI-D-12-00022.1.

Cook, B.I., Seager, R., Smerdon, J.E., 2014. The worst North American drought year of the last millennium: 1934. Geophys. Res. Lett. 41 (20), 7298–7305. doi:http://dx.doi.org/10.1002/2014GL061661.

Cook, B.I., Ault, T.R., Smerdon, J.E., 2015. Unprecedented 21st century drought risk in the American Southwest and Central Plains. Sci. Adv. 1 (1) doi:http://dx.doi.org/10.1126/sciadv.1400082 e1400082–e1400082.

Cook, E.R., Seager, R., Cane, M.A., Stahle, D.W., 2007. North American drought: reconstructions, causes, and consequences. Earth-Sci. Rev. 81 (1–2), 93–134. doi:http://dx.doi.org/10.1016/j.earscirev.2006.12.002.

Cordova, C., Porter, J.C., 2015. The 1930s Dust Bowl: geoarchaeological lessons from a 20th century environmental crisis. Holocene 25, 1707–1720.

Cowan, T., Hegerl, G.C., Colfescu, I., Bollasina, M., Purich, A., Boschat, G., 2017. Factors contributing to record-breaking heat waves over the Great Plains during the 1930s dust bowl. J. Clim. 30 (7), 2437–2461. doi:http://dx.doi.org/10.1175/JCLI-D-16-0436.1.

Cronin, F.D., Beers, H.W., 1937. Areas of Intense Drought Distress 1930-1936. Works Progress Administration, Division of Social Research, Washington, D.C, pp. 54.

Crouvi, O., Schepanski, K., Amit, R., Gillespie, A.R., Enzel, Y., 2012. Multiple dust sources in the Sahara Desert: the importance of sand dunes. Geophys. Res. Lett. 39, L13401.

Cunfer, G., 2005. On the Great Plains: Agriculture and Environment. Texas A&M University Press, College Station, TX, pp. 292.

Disterdick, F.L., 1933. Severe sand storm in eastern Wyoming, January 18, 1933. Mon. Weather Rev 61, 16–17.

Donarummo, J., 2003. Possible deposit of soil dust from the 1930's U.S. dust bowl identified in Greenland ice. Geophys. Res. Lett. 30 (6) doi:http://dx.doi.org/10.1029/2002GL016641.

Donat, M.G., King, A.D., Overpeck, J.T., Alexander, L.V., Durre, I., Karoly, D.J., 2016. Extraordinary heat during the 1930s US Dust Bowl and associated large-scale conditions. Clim. Dyn. 46 (1–2), 413–426. doi:http://dx.doi.org/10.1007/s00382-015-2590-5.

Duncan, D., Burns, K., 2012. The Dust Bowl: An Illustrated History. Chronicle Books, San Francisco, CA, pp. 232.

Eagar, J.D., Herckes, P., Hartnett, H.E., 2017. The characterization of haboobs and the deposition of dust in Tempe, AZ from 2005 to 2014. Aeolian Res. 24, 81–91. doi: http://dx.doi.org/10.1016/j.aeolia.2016.11.004.

Eby, L.K., Whitfield, C.J., 1940. Soil and erosion changes on the dalhart sand dune area. J. Am. Soc. Agron. 32 (4), 290–296.

Egan, T., 2006. The Worst Hard Time: the Untold Story of Those Who Survived the Great American Dust Bowl. Houghton Mifflin Harcourt, New York, pp. 340.

Engelstaedter, S., Tegen, I., Washington, R., 2006. North African dust emissions and transport. Earth-Sci. Rev. 79 (1–2), 73–100. doi:http://dx.doi.org/10.1016/j.earscirev.2006.06.004.

Etyemezian, V., Nikolich, G., Ahonen, S., Pitchford, M., Sweeney, M., Purcell, R., et al., 2007. The Portable in Situ Wind Erosion laboratory (PI-SWERL): a new method to measure PM10 windblown dust properties and potential for emissions. Atmos. Environ. 41 (18), 3789–3796.

Etyemezian, V., Gillies, J.A., Shinoda, M., Nikolich, G., King, J., Bardis, A.R., 2014. Accounting for surface roughness on measurements conducted with PI-SWERL: evaluation of a subjective visual approach and a photogrammetric technique. Aeolian Res. 13, 35–50.

Flagg, C.B., Neff, J.C., Reynolds, R.L., Belnap, J., 2014. Spatial and temporal patterns of dust emissions (2004–2012) in semi-arid landscapes, southeastern Utah, USA. Aeolian Res. 15, 31–43. doi:http://dx.doi.org/10.1016/j.aeolia.2013.10.002.

Forman, S.L., Oglesby, R., Webb, R.S., 2001. Temporal and spatial patterns of Holocene dune activity on the Great Plains of North America: megadroughts and climate links. Glob. Planet. Change 29, 1–29.

Forman, S.L., Marín, L., Gomez, J., Pierson, J., 2008. Late Quaternary eolian sand depositional record for southwestern Kansas: landscape sensitivity to droughts. Palaeogeogr. Palaeoclimatol. Palaeoecol. 265 (1–2), 107–120. doi:http://dx.doi.org/10.1016/j.palaeo.2008.04.028.

Fye, F.K., Stahle, D.W., Cook, E.R., Cleaveland, M.K., 2006. NAO influence on sub-decadal moisture variability over central North America. Geophys. Res. Lett. 33 (15) doi:http://dx.doi.org/10.1029/2006GL026656.

Geiger, R., 1935. Oklahoma battles another severe dust storm. The Evening Star. W.D. Wallach and Hope, Washington, D.C, pp. A-2 June 15, 1935.

General Records of the Soil Erosion Service and the Soil Conservation Service, 1915–77, Record Group 114; National Archives at College Park, College Park, MD.

Gherardi, L.A., Sala, O.E., 2015. Enhanced precipitation variability decreases grass- and increases shrub-productivity. Proc. Natl. Acad. Sci. U. S. A. 112, 12735–12740.

Gillette, D.A., 1979. Environmental factors affecting dust emission by wind erosion. In: Morales, C. (Ed.), Saharan Dust. John Wiley, New York, pp. 71–94.

Gillette, D.A., 1988. Threshold friction velocities for dust production for agricultural soils. J. Geophys. Res. 93, 12645–12662 D10.

Gillette, D.A., Adams, J., Endo, A., Smith, D., Kihl, R., 1980. Threshold velocities for input of soil particles into the air by desert soils. J. Geophys. Res. 85 (C10), 5621–5630.

Gillette, D.A., Adams, J., Muhs, D., Kihl, R., 1982. Threshold friction velocities and rupture moduli for crusted desert soils for the input of soil particles into the air. J. Geophys. Res. 87 (C11), 9003–9015.

Ginoux, P., Prospero, J.M., Gill, T.E., Hsu, N.C., Zhao, M., 2012. Global-scale attribution of anthropogenic and natural dust sources and their emission rates based on MODIS Deep Blue aerosol products. Rev. Geophys. 50 (3) doi:http://dx.doi.org/10.1029/2012RG000388.

Gkikas, A., Hatzianastassiou, N., Mihalopoulos, N., Katsoulis, V., Kazadzis, S., Pey, J., 2013. The regime of desert dust episodes in the Mediterranean based on contemporary satellite observations and ground measurements. Atmos. Chem. Phys. 13, 12135–12154.

Goossens, D., Buck, B., 2009. Dust emission by off-road driving: experiments on 17 arid soil types, Nevada, USA. Geomorphology 107 (3-4), 118–138.

Goossens, D., Buck, B., 2011. Gross erosion, net erosion and gross deposition of dust by wind: field data from 17 desert surfaces. Earth Surf. Process. Landf. 36 (5), 610–623. doi:http://dx.doi.org/10.1002/esp.2080.

Goudie, A.S., 2014. Desert dust and human health disorders. Env. Internat. 63, 101–113.

Hahnenberger, M., Nicoll, K., 2012. Meteorological characteristics of dust storm events in the eastern Great Basin of Utah, U.S.A. Atmos. Environ. 60, 601–612. doi:http://dx.doi.org/10.1016/j.atmosenv.2012.06.029.

Hand, I.F., 1934. The character and magnitude of the dense dust-cloud which passed over Washington, DC, May 11, (1934). Mon. Weather Rev. 62, 156.

Handy, R.L., Lyon, C.A., Davidson, D.T., 1960. Analysis of wind-blown silt. Geologic and Engineering Properties of Pleistocene Materials. Iowa State University Joint Publication Bulletin No. 191, Iowa State University, Iowa City, Iowa, pp. 1–13.

Hansen, Z.K., Libecap, G.D., 2004. Small farms, externalities, and the Dust Bowl of the 1930s. J. Polit. Econ. 112 (5), 665–694.

Hanson, P.R., Arbogast, A.F., Johnson, W.C., Joeckel, R.M., Young, A.R., 2010. Megadroughts and late Holocene dune activation at the eastern margin of the Great Plains, north-central Kansas, USA. Aeolian Res. 1 (3-4), 101–110.

Hegerl, G.C., Brönnimann, S., Schurer, A., Cowan, T., 2018. The early 20th century warming: anomalies, causes, and consequences. Wiley Interdiscip. Rev. Clim. Change 9 (4), e522.

Higgins, R.W., Yao, Y., Wang, X.L., 1997. Influence of the North American monsoon system on the US summer precipitation regime. J. Clim. 10 (10), 2600–2622.

Hong, S.-Y., Kalnay, E., 2000. Role of sea surface temperature and soil-moisture feedback in the 1998 Oklahoma–Texas drought. Nature 408 (6814), 842–844.

Hornbeck, R., 2012. The enduring impact of the american dust bowl: short- and long-run adjustments to environmental catastrophe. Am. Econ. Rev. 102 (4), 1477–1507. doi:http://dx.doi.org/10.1257/aer.102.4.1477.

Houser, C., Bishop, M.P., Barrineau, P., 2015. Characterizing instability of aeolian environments using analytical reasoning: analytical reasoning of aeolian instability. Earth Surf. Process. Landf. 40 (5), 696–705. doi:http://dx.doi.org/10.1002/esp.3679.

Hovde, M.R., 1934. The great dust storm of November 12, 1933. Mon. Weather Rev. 62, 12–13.

Hu, Q., Torres-Alavez, J.A., Van Den Broeke, M.S., 2018. Land-cover change and the "Dust bowl" drought in the US Great Plains. J. Clim. 31 (12), 4657–4667.

Huang, Y., Kok, J.F., Martin, R.L., Swet, N., Katra, I., Gill, T.E., Reynolds, R.L., Freire, L.S., 2019. Fine dust emissions from active sands at coastal Oceano Dunes, California. Atmos. Chem. Phys. 19, 2947–2964. doi:http://dx.doi.org/10.5194/acp-19-2947-2019.

Hugenholtz, C.H., Wolfe, S.A., 2005. Biogeomorphic model of dunefield activation and stabilization on the northern Great Plains. Geomorphology 70 (1–2), 53–70. doi:http://dx.doi.org/10.1016/j.geomorph.2005.03.011.

Hurt, R.D., 1981. The Dust Bowl: An Agricultural and Social History. Taylor Trade Publications, Chicago, pp. 214.

Idso, S.B., Ingram, R.S., Pritchard, J.M., 1972. An American Haboob. B. Am. Meteorol. Soc 53, 930–955.

Jickells, T.D., 2005. Global Iron connections between desert dust, ocean biogeochemistry, and climate. Science 308 (5718), 67–71. doi:http://dx.doi.org/10.1126/science.1105959.

Joel, A.H., 1937. Soil Conservation Reconnaissance Survey of the Southern Great Plains Wind-erosion Area (Technical Bulletin No. 556). U.S. Department of Agriculture, Washington, D.C.

Johnson, V., 1947. Heaven's Tableland. Da Capo Press, New York, pp. 288.

King, J., Etyemezian, V., Sweeney, M., Buck, B.J., Nikolich, G., 2011. Dust emission variability at the Salton Sea, California, USA. Aeolian Res. 3 (1), 67–79. doi:http://dx.doi.org/10.1016/j.aeolia.2011.03.005.

Knippertz, P., 2014. Meteorological aspects of dust storms. Mineral Dust. Springer, Dordrecht, pp. 121–147.

Lancaster, N., 1985. Variations in wind velocity and sand transport on the windward flanks of desert sand dunes. Sedimentology 32 (4), 581–593.

Lancaster, N., 2004. Relations between aerodynamic and surface roughness in a hyper-arid cold desert: McMurdo Dry Valleys, Antarctica. Earth Surf. Process. Landf. 29 (7), 853–867.

Lange, D., 1981. Dorothea Lange: Farm Security Administration Photographs, 1935-1939 (Dorothea Lange), Volume II. Tech-Fiche Press, pp. 236.

Langham, W.H., Foster, R.L., Daniel, H.A., 1938. The amount of dust in the air at plant height during wind storms at Goodwell, Oklahoma in 1936-1937. J. Am. Soc. Agron. 30, 139–144.

Lee, J.A., Gill, T.E., 2015. Multiple causes of wind erosion in the Dust Bowl. Aeolian Res. 19, 15–36. doi:http://dx.doi.org/10.1016/j.aeolia.2015.09.002.

Lee, J.A., Tchakerian, V.P., 1995. Magnitude and frequency of blowing dust on the Southern High Plains of the United States, 1947-1989. Ann. Assoc. Am. Geogr. 85 (4), 684–693.

Lee, J.A., Gill, T.E., Mulligan, K.R., Dominguez Acosta, M., Perez, A.E., 2009. Land use/land cover and point sources of the 15 December 2003 dust storm in southwestern North America. Geomorphology 105 (1–2), 18–27. doi:http://dx.doi.org/10.1016/j.geomorph.2007.12.016.

Lee, J.A., Baddock, M.C., Mbuh, M.J., Gill, T.E., 2012. Geomorphic and land cover characteristics of aeolian dust sources in West Texas and eastern New Mexico, USA. Aeolian Res. 3 (4), 459–466. doi:http://dx.doi.org/10.1016/j.aeolia.2011.08.001.

Lei, H., Wang, J.X.L., 2014. Observed characteristics of dust storm events over the western United States using meteorological, satellite, and air quality measurements. Atmos. Chem. Phys. 14 (15), 7847–7857. doi:http://dx.doi.org/10.5194/acp-14-7847-2014.

Lockeretz, W., 1978. Lessons of the dust bowl. Am. Sci. 66, 560–569.

Lookingbill, B.D., 2001. Dust Bowl, USA: Depression America and the Ecological Imagination, 1929-1941. Ohio University Press, Athens, OH, pp. 190.

Maddox, R.A., 1983. Large-scale meteorological conditions associated with midlatitude, mesoscale convective complexes. Mon. Weather. Rev. 111 (7), 1475–1493.

Mallone, S., Stafoggia, M., Faustini, A., Gobbi, G.P., Marconi, A., Forastiere, F., 2011. Saharan Dust and Associations between Particulate Matter and Daily Mortality in Rome, Italy. Environ. Health Perspect. 119 (10), 1409–1414. doi:http://dx.doi.org/10.1289/ehp.1003026.

Mangan, J.M., Overpeck, J.T., Webb, R.S., Wessman, C., Goetz, A.F., 2004. Response of Nebraska Sand Hills natural vegetation to drought, fire, grazing, and plant functional type shifts as simulated by the CENTURY model. Clim. Change 63 (1–2), 49–90.

Martin, R.J., 1936a. Dust storms in the United States, April 1936. Mon. Weather Rev. 64, 137.

Martin, R.J., 1936b. Dust storms of may 1936 in the United States. Mon. Weather Rev. 64, 176.

Martin, R.J., 1936c. Dust storms of July 1936 in the United States. Mon. Weather Rev. 64, 239.

Martin, R.J., 1938. Dust storms of may-december 1937 in the United States. Mon. Weather Rev. 66, 9.

Mattice, W.A., 1935a. Dust storms, November 1933 to may 1934. Mon. Weather Rev. 63, 53–55.

Mattice, W.A., 1935b. Dust storms. Mon. Weather Rev. 63, 113–115.

McDowell, N.G., 2011. Mechanisms linking drought, hydraulics, carbon metabolism, and vegetation mortality. Plant Physiol. 155 (3), 1051–1059.

Menne, M.J., Durre, I., Vose, R.S., Gleason, B.E., Houston, T.G., 2012. An overview of the global historical climatology network-daily database. J. Atmos. Oceanic Technol. 29, 897–910. doi:http://dx.doi.org/10.1175/JTECH-D-11-00103.1.

Miao, X., Mason, J.A., Swinehart, J.B., Loope, D.B., Hanson, P.R., Goble, R.J., Liu, X., 2007. A 10,000 year record of dune activity, dust storms, and severe drought in the central Great Plains. Geology 35 (2), 119–122.

Miller, E.R., 1934. The dustfall of November 12-13, 1933. Mon. Weather Rev. 62, 14–15.

Mo, K.C., Paegle, J.N., Higgins, R.W., 1997. Atmospheric processes associated with summer floods and droughts in the central United States. J. Climate 10, 3028–3046.

Moran, M.S., Ponce-campos, G.E., Huete, A.R., McClaran, M.P., 2014. Functional response of U.S. Grasslands to the early 21st-century drought. Ecology 95 (8), 2121–2133.

Morman, S.A., Plumlee, G.S., 2013. The role of airborne mineral dusts in human disease. Aeolian Res. 9, 203–212. doi:http://dx.doi.org/10.1016/j.aeolia.2012.12.001.

Namias, J., 1982. Anatomy of Great Plains protracted heat waves especially in the 1980 U.S. Summer drought. Mon. Weather Rev 110, 824–838.

Namias, J., 1990. Spring and summer 1988 drought over the contiguous United States-causes and prediction. J. Climate 4, 54–65.

Nandintsetseg, B., Shinoda, M., 2015. Land surface memory effects on dust emission in a Mongolian temperate grassland: land surface memory effects on dust. J. Geophys. Res. Biogeosci. 120 (3), 414–427. doi:http://dx.doi.org/10.1002/2014JG002708.

Natsagdorj, L., Jugder, D., Chung, Y.S., 2003. Analysis of dust storms observed in Mongolia during 1937–1999. Atmos. Environ. 37 (9-10), 1401–1411.

Nickling, W.G., Gillies, J.A., 1989. Emission of fine-grained particulates from desert soils. In: Leinen, M., Sarnthein, M. (Eds.), Paleoclimatology and Paleometeorology: Modern and Past Patterns of Global Atmospheric Transport. Kluwer Academic Publishers, pp. 133–165.

Nicoll, K.A., Harrison, R.G., Ulanowski, Z., 2011. Observations of Saharan dust layer electrification. Environ. Res. Lett. 6, 014001.

Nigam, S., Guan, B., Ruiz-Barradas, A., 2011. Key role of the Atlantic Multidecadal Oscillation in 20th century drought and wet periods over the Great Plains. Geophys. Res. Lett. 38, L16713.

Novlan, D.J., Hardiman, M., Gill, T.E., 2007. A synoptic climatology of blowing dust events in El Paso, Texas from 1932-2005. 87th AMS Annual Meeting J3.12.

Ohm, K.B., 1980. Dorthea Lange and the Documentary Tradition. Louisiana State University Press, Baton Rouge, LA, pp. 277.

Oke, T.R., 1978. Boundary Layer Climates. Methuen and Co Ltd, London, pp. 372.

Orgill, M.M., Sehmel, G.A., 1976. Frequency and diurnal-variation of dust storms in Contiguous USA. Atmos. Environ. 10, 813–825.

Packer, G., 2011. Photographs of Arthur Rothstein: The Library of Congress. D. Giles Ltd, UK, pp. 154.

Parajuli, S.P., Yang, Z.-L., Kocurek, G., 2014. Mapping erodibility in dust source regions based on geomorphology, meteorology, and remote sensing: land cover and erodibility mapping. J. Geophys. Res. Earth Surf. 119 (9), 1977–1994. doi:http://dx.doi.org/10.1002/2014JF003095.

Patterson, E.M., Gillette, D.A., 1976. Measurements of Visible and Infrared Imagery Index of Refraction and of Size Distribution for Saharan Dust Aerosols over Atlantic. B. Am. Meteorol. Soc. 57 146-146.

Peters, D.P., Pielke, R.A., Bestelmeyer, B.T., Allen, C.D., Munson-McGee, S., Havstad, K. M., 2004. Cross-scale interactions, nonlinearities, and forecasting catastrophic events. Proc. Natl. Acad. Sci. U. S. A. 101 (42), 15130–15135.

Peters, D.P.C., Osvaldo, E.S., Allen, C.D., Covich, A., Brunson, M., 2007. Cascading events in linked ecological and socioeconomic systems. Front. Ecol. Environ. 5 (4), 221–224.

Peters, D.P.C., Havstad, K.M., Archer, S.R., Sala, O.E., 2015. Beyond desertification: new paradigms for dryland landscapes. Front. Ecol. Environ. 13, 4–12.

Porter, J., Finchum, G.A., 2009. Redefining the dust bowl region via popular perception and geotechnology. Great Plains Res 19, 201–214.

Porter, J., 2012. Lessons from the dust bowl: human-environment education on the Great Plains. J. Geogr. 111, 127–136.

Pu, B., Ginoux, P., 2017. Projection of American dustiness in the late 21st century due to climate change. Sci. Rep. 7 (1) doi:http://dx.doi.org/10.1038/s41598-017-05431-9.

Pu, B., Ginoux, P., 2018. Climatic factors contributing to long-term variations in surface fine dust concentration in the United States. Atmos. Chem. Phys. 18 (6) .

Qian, W.H., Tang, X., Quan, L.S., 2004. Regional characteristics of dust storms in China. Atmos. Environ. 38, 4895–4907.

Raman, A., Arellano, A.F., Brost, J.J., 2014. Revisiting haboobs in the southwestern United States: an observational case study of the 5 July 2011 Phoenix dust storm. Atmos. Environ. 89, 179–188. doi:http://dx.doi.org/10.1016/j.atmosenv.2014.02.026.

Ravi, S., Breshears, D.D., Huxman, T.E., D'Odorico, P., 2010. Land degradation in drylands: interactions among hydrologic–aeolian erosion and vegetation dynamics. Geomorphology 116 (3–4), 236–245. doi:http://dx.doi.org/10.1016/j.geomorph.2009.11.023.

Rendón, A.M., Salazar, J.F., Palacio, C.A., Wirth, V., 2015. Temperature inversion breakup with impacts on air quality in urban valleys influenced by topographic shading. J. Appl. Meteorol. Climatol. 54 (2), 302–321. doi:http://dx.doi.org/10.1175/JAMC-D-14-0111.1.

Riebsame, W.E., 1986. The dust bowl historical image, psychological anchor, and ecological taboo. Great Plains Quart. 6, 127–136.

Rivera Rivera, N.I., Gill, T.E., Gebhart, K.A., Hand, J.L., Bleiweiss, M.P., Fitzgerald, R.M., 2009. Wind modeling of Chihuahuan Desert dust outbreaks. Atmos. Environ. 43 (2), 347–354.

Rivera Rivera, N.I., Gill, T.E., Bleiweiss, M.P., Hand, J.L., 2010. Source characteristics of hazardous Chihuahuan Desert dust outbreaks. Atmos. Environ. 44 (20), 2457–2468. doi:http://dx.doi.org/10.1016/j.atmosenv.2010.03.019.

Schlesinger, W.H., Reynolds, J.F., Cunningham, G.L., Huenneke, L.F., Jarrell, W.M., Virginia, R.A., Whitford, W.G., 1990. Biological feedbacks in global desertification. Science 247 (4946), 1043–1048.

Schmeisser, R.L., Loope, D.B., Mason, J.A., 2010. Modern and late Holocene wind regimes over the Great Plains (central U.S.A.). Quat. Sci. Rev. 29 (3–4), 554–566. doi:http://dx.doi.org/10.1016/j.quascirev.2009.11.003.

Schubert, S., Suarez, M., Pegion, P., Koster, R., Bacmeister, J., 2004. On the cause of the 1930s dust bowl. Science 303 (5665), 1855–1859.

Seager, R., Hoerling, M., 2014. Atmosphere and Ocean Origins of North American Droughts. J. Clim. 27 (12), 4581–4606. doi:http://dx.doi.org/10.1175/JCLI-D-13-00329.1.

Seager, R., Burgman, R., Kushnir, Y., Clement, A., Cook, E., Naik, N., Miller, J., 2008. Tropical pacific forcing of north american medieval megadroughts: testing the concept with an atmosphere model forced by coral-reconstructed SSTs. J. Clim. 21 (23), 6175–6190. doi:http://dx.doi.org/10.1175/2008JCLI2170.1.

Shao, Y., Raupach, M.R., Findlater, P.A., 1993. Effect of saltation bombardment on the entrainment of dust by wind. J. Geophys. Res. Atmos. 98 (D7), 12719–12726.

Sidwell, R., 1938. Sand and dust storms in vicinity of Lubbock, Texas. Econ. Geog 14, 98–102.

Smith, R.M., Twiss, P.C., Krauss, R.K., Brown, M.J., 1970. Dust Deposition in Relation to Site, Season, and Climatic Variables. The Soil and Water Conservation Research Division, Department of Agronomy Contribution no. 1076, Kansas Agricultural Experimental Station, Manhattan, KS, pp. 112–117.

Soil Survey Staff, 2019. Natural Resources Conversation Service, United States Department of Agriculture. Official Soil Series Descriptions Available online. Accessed [06/14/2019].

Sow, M., Crase, E., Rajot, J.L., Sankaran, R.M., Lacks, D.J., 2011. Electrification of particles in dust storms: field measurements during the monsoon period in Niger. Atm. Res. 102, 343–350.

Sprigg, W.A., Nickovic, S., Galgiani, J.N., Pejanovic, G., Petkovic, S., Vujadinovic, M., et al., 2014. Regional dust storm modeling for health services: the case of valley fever. Aeolian Res. 14, 53–73. doi:http://dx.doi.org/10.1016/j.aeolia.2014.03.001.

Sridhar, V., Loope, D.B., Swinehart, J.B., Mason, J.A., Oglesby, R.J., Rowe, C.M., 2006. Large wind shift on the Great Plains during the medieval warm period. Science 313 (5785), 345–347.

Stafoggia, M., Zauli-Sajani, S., Pey, J., Samoli, E., Alessandrini, E., Basagana, X., Cernigliaro, et al., 2016. Desert dust outbreaks in southern europe: contribution to daily PM10 concentrations and short-term associations with mortality and hospital admissions. Environ. Health Perspect. 124, 413–419.

Stahle, D.W., Fye, F.K., Cook, E.R., Griffin, R.D., 2007. Tree-ring reconstructed megadroughts over North America since AD 1300. Clim. Change 83 (1-2), 133.

Stallings, F.L., 2001. Black Sunday: the Great Dust Storm of April 14, 1935. Eakin Press.

Su, H., Yang, Z.-L., Dickinson, R.E., Wei, J., 2014. Spring soil moisture-precipitation feedback in the Southern Great Plains: How is it related to large-scale atmospheric conditions? Geophys. Res. Lett. 41 (4), 1283–1289. doi:http://dx.doi.org/10.1002/2013GL058931.

Sutton, L.J., 1931. Haboobs. Q. J. R. Meteorol. Soc. 57, 143–161.

Svejcar, L.N., Bestelmeyer, B.T., Duniway, M.C., James, D.K., 2015. Scale–Dependent feedbacks between patch size and plant reproduction in Desert Grassland. Ecosystems 18 (1), 146–153.

Sweeney, M.R., Mason, J.A., 2013. Mechanisms of dust emission from Pleistocene loess deposits, Nebraska, USA. J. Geophys. Res. Earth Surf. 118 (3), 1460–1471.

Sweeney, M.R., Etyemezian, V., Macpherson, T., Nickling, W., Gillies, J., Nikolich, G., McDonald, E., 2008. Comparison of PI-SWERL with dust emission measurements from a straight-line field wind tunnel. J. Geophys. Res. Earth Surf. 113 (F1) .

Sweeney, M.R., McDonald, E.V., Etyemezian, V., 2011. Quantifying dust emissions from desert landforms, eastern Mojave Desert, USA. Geomorphology 135 (1–2), 21–34. doi:http://dx.doi.org/10.1016/j.geomorph.2011.07.022.

Sweeney, M.R., Lu, H., Cui, M., Mason, J.A., Feng, H., Xu, Z., 2016a. Sand dunes as potential sources of dust in northern China. Sci. China Earth Sci. 59 (4), 760–769.

Sweeney, M.R., Zlotnik, V.A., Joeckel, R.M., Stout, J.E., 2016b. Geomorphic and hydrologic controls of dust emissions during drought from Yellow Lake playa, West Texas, USA. J. Arid Environ. 133, 37–46.

Swet, N., Elperin, T., Kok, J.F., Martin, R.L., Yizhaq, H., Katra, I., 2019. Can active sands generate dust particles by wind-induced processes? Earth Planet. Sci. Lett. 506, 371–380.

Sylvester, K.M., Rupley, E.S.A., 2012. Revising the dust bowl: high above the Kansas Grasslands. Environ. Hist. 17 (3), 603–633. doi:http://dx.doi.org/10.1093/envhis/ems047.

Tai, A.P.K., Mickley, L.J., Jacob, D.J., Leibensperger, E.M., Zhang, L., Fisher, J.A., Pye, H.O. T., 2012. Meteorological modes of variability for fine particulate matter (PM2.5) air quality in the United States: implications for PM2.5 sensitivity to climate change. Atmos. Chem. Phys. 12 (6), 3131–3145. doi:http://dx.doi.org/10.5194/acp-12-3131-2012.

Takaro, T.K., Henderson, S.B., 2015. Climate change and the new normal for cardiorespiratory disease. Can. Respir. J. 22 (1), 52–54.

Takaro, T.K., Knowlton, K., Balmes, J.R., 2013. Climate change and respiratory health: current evidence and knowledge gaps. Expert Rev. Respir. Med. 7 (4), 349–361. doi:http://dx.doi.org/10.1586/17476348.2013.814367.

Tegen, I., Lacis, A.A., Fung, I., 1996. The influence on climate forcing of mineral aerosols from disturbed soils. Nature 380 (6573), 419–422. doi:http://dx.doi.org/10.1038/380419a0.

Tong, D.Q., Wang, J.X.L., Gill, T.E., Lei, H., Wang, B., 2017. Intensified dust storm activity and Valley fever infection in the southwestern United States: dust and Valley Fever Intensification. Geophys. Res. Lett. 44 (9), 4304–4312. doi:http://dx.doi.org/10.1002/2017GL073524.

Turnure, R.F., 1938. Soil Associations of the United States. Map, Scale 1:63360. Soils Survey Division, United States.

Veste, M., Littmann, T., Breckle, S.W., Yair, A., 2001. The role of biological soil crusts on desert sand dunes in the northwestern Negev, Israel. Sustainable Land Use in Deserts. Springer, Berlin, Heidelberg, pp. 357–367.

Vivoni, E.R., Tai, K., Gochis, D.J., 2009. Effects of initial soil moisture on rainfall generation and subsequent hydrologic response during the North American monsoon. J. Hydrometeorol. 10 (3), 644–664. doi:http://dx.doi.org/10.1175/2008JHM1069.1.

Warn, G.F., 1952. Some dust storm conditions of the southern high plains. Bull. Am. Meteorol. Soc. 33 (6), 240–243.

Werner, C.M., Mason, J.A., Hanson, P.R., 2011. Non-linear connections between dune activity and climate in the High Plains, Kansas and Oklahoma, USA. Quat. Res. 75 (1), 267–277. doi:http://dx.doi.org/10.1016/j.yqres.2010.08.001.

Whitfield, C.J., 1938. Sand dunes of recent origin in southern Great Plains. J. Agric. Res. 56 (12), 907–917.

Wiggs, G.F.S., Livingstone, I., Thomas, D.S.G., Bullard, J.E., 1994. Effect of vegetation removal on airflow patterns and dune dynamics in the southwest Kalahari Desert. Land Degrad. Dev. 5 (1), 13–24.

Wigner, K.A., Peterson, R.E., 1987. Synoptic climatology of blowing dust on the Texas South Plains, 1947-84. J. Arid Environ. 13 (3), 199–209.

Wilks, D.S., 2011. Statistical Methods in the Atmospheric Sciences, third edition Academic Press, New York.

Williams, E.R., 2007. Comment on "Atmospheric controls on the annual cycle of North African dust" by S. Engelstaedter and R. Washington. J. Geophys. Res. Atmos. 113, D23109.

Williams, E.R., Nathou, N., Hicks, E., Pontikis, C., Russell, B., Miller, M., Bartholomew, M.J., 2009. The electrification of dust-lofting gust fronts ('haboobs') in the Sahel. Atm. Res. 91, 292–298.

Woodhouse, C.A., Meko, D.M., MacDonald, G.M., Stahle, D.W., Cook, E.R., 2010. A 1,200-year perspective of 21st century drought in southwestern North America. Proc. Natl. Acad. Sci. 107 (50), 21283–21288. doi:http://dx.doi.org/10.1073/pnas.0911197107.

Woodhouse, C.A., Overpeck, J.T., 1998. 2000 years of drought variability in the central United States. Bull. Am. Meteorol. Soc. 79 (12), 2693–2714.

Worster, D., 1979. Dust Bowl: The Southern Plains in the 1930s. Oxford University Press, New York, pp. 290.

Xu, J., Shuttleworth, W.J., Gao, X., Sorooshian, S., Small, E.E., 2004. Soil moisture–precipitation feedback on the North American monsoon system in the MM5-OSU model. Q. J. R. Meteorol. Soc. 130 (603), 2873–2890. doi:http://dx.doi.org/10.1256/qj.03.192.

Yair, Y., Katz, S., Yaniv, R., Ziv, B., Price, C., 2016. An electrified dust storm over the Negev desert, Israel. Atm. Res. 181, 63–71.